Report
P-21-26
April 2022

UNTAMO model description

Model version 3.5

Martin Gunia
Katja Gunia

SVENSK KÄRNBRÄNSLEHANTERING AB

SWEDISH NUCLEAR FUEL
AND WASTE MANAGEMENT CO

Box 3091, SE-169 03 Solna
Phone +46 8 459 84 00
skb.se

SVENSK KÄRNBRÄNSLEHANTERING

ISSN 1651-4416
SKB P-21-26
ID 1963456

April 2022

UNTAMO model description

Model version 3.5

Martin Gunia, Katja Gunia
Arbonaut Ltd

Summary

The purpose of this report is to document and present the mechancis of the UNTAMO software package: a modelling tool used for simulating the evolution of landscapes over long periods of times. The development of the software started in 2006 and the software has been continuously maintained and developed up to the publishing of this report. The current version of the software is 3.5. The report describes the conceptual design of the landscape evolution model, the specific ecosystems that are considered in the evolution of the landscape, and the processes that drive the evolution in the landscape. A mathematical description of the individual conceptual models used within UNTAMO is given when appropriate. Flow charts are used to visually present the individual algorithms which make up UNTAMO. Input data sets required to run the software and the output datasets produced by the software are presented in the report. The documentation of the UNTAMO model (i.e. this report) is seen as an ongoing process and it is expected that this report will be revised and complemented over time.

Sammanfattning

Syftet med denna rapport är att dokumentera och redovisa mjukvarupaketet UNTAMO: ett modelleringsverktyg som används för simulering av landskapets utveckling över långa tidsperioder. Utvecklingen av mjukvaran påbörjades 2006 och har sedan dess uppdaterats kontinuerligt och vidareutvecklats fram till publiceringen av denna rapport. Mjukvarans aktuella version är 3.5. Denna rapport beskriver den konceptuella designen av landskapsutvecklingsmodellen, de specifika ekosystemen som beaktas i landskapets utveckling, och processerna som driver evolutionen av landskapet. En matematisk beskrivning av de individuella konceptuella modeller som används inom UNTAMO redovisas om det anses lämpligt. Flödesscheman används för att visualisera de individuella algoritmer som utgör UNTAMO. Indata som krävs för att köra mjukvaran samt utdata som produceras av mjukvaran redovisas i rapporten. Dokumentation av UNTAMO-modellen (d.v.s. denna rapport) anses vara en levande process och det antas att denna rapport kommer att revideras och kompletteras över tid.

Contents

1 Introduction

UNTAMO Toolbox (further just UNTAMO) is a set of GIS processing tools and an environment for modelling of evolution of landscape and ecosystems. The focus is on long time scales, typically over several thousands of years, and the toolbox is suitable for temperate conditions. In particular, the tool is not suitable for modelling of landscape that is covered with an ice sheet during a glacial period.

The UNTAMO landscape and ecosystems evolution model is an empirical model that relies on model calibration to obtain suitable parameter values. This is motivated by the fact that physical models would require long running times for the spatial domains that need to be modelled and given the long time scales being modelled. Representative parameter values may also not be available for physical models.

The Regolith Lake Development Model (RLDM), developed by Brydsten and Strömgren (2013) at the Swedish Nuclear Fuel and Waste Management Co (SKB) is the predecessor to UNTAMO. One major difference between UNTAMO and the RLDM is that UNTAMO integrates all models of landscape and ecosystems evolution within the main time-stepping loop, rather than modelling these processes separately as was done in the RLDM. Also, UNTAMO is, at the time of writing, under active development while RLDM development has ended.

This document describes the current state of the UNTAMO software. The document will be continuously updated to reflect changes and improvements made to the UNTAMO software. The document is organized so that Chapter 2 contains description of conceptual and mathematical models implemented in UNTAMO and Chapter 3 presents input and output data. Chapter 4 discusses the software limitation and potential areas of improvement. Detailed parameter documentation is currently outside of the scope of this document but may be added in future versions.

1.1 Version history

UNTAMO has been commissioned in 2006 by Posiva Ltd. to support Posiva's spent nuclear disposal safety case (Hjerpe et al. 2010) and has been continuously developed and maintained. Version 1 of the software consisted of individual geo-processing tools for ArcGIS software whose aim was to perform common tasks encountered during the landscape evolution modelling work. Development of version 2 started in 2010 and integrated existing tools and modules into a "landscape and ecosystem evolution model" with a time-stepping loop over the entire modelled time frame. As in version 1, the models were written for ArcGIS in the C# language. UNTAMO version 2 has been used in Posiva's Biosphere Assessment 2012 modelling (Posiva 2013). Development on version 3 started in 2014, based on earlier feedback. The software has been rewritten in C++ and the use of ArcGIS has been dropped for performance and reliability reasons. Numerous modules have been added and improved, including the sediment accumulation and resuspension module, cropland allocation module and biosphere object delineation functionality.

2 Conceptual and mathematical models

2.1 Landscape evolution overview

This chapter presents conceptual models of the landscape features and processes that are handled in UNTAMO as well as their mathematical implementation. Where feasible, the implemented algorithms are visualized using flowcharts. The legend for all flowcharts is shown in Figure 2-1 and is not repeated in later sections.

UNTAMO produces a series of "snapshots" which describe the state of the landscape and ecosystems at time steps defined by the user. Given a snapshot at the previous time t_{k-1}, the snapshot at a time t_k, $t_k > t_{k-1}$ is computed by first applying models of processes such as the shoreline displacement or sediment accumulation and resuspension over the period $\Delta t = t_k - t_{k-1}$. After the state of the landscape and ecosystems has been "propagated" to the time t_k, features of the landscape are identified and the time-stepping loop continues with the next iteration. The time-stepping loop of UNTAMO is illustrated in Figure 2-2.

It should be noted that some landscape changes are also applied during the feature identification stage. This is true for processes that are assumed to be shorter than the time stepping interval and thus do not need to be modelled as functions of time. Instead, they are applied immediately during feature identification. One such example is the river incision process, which is applied immediately after a river has been identified.

The individual computational steps performed for one time-stepping iteration are shown in Figure 2-3 (process models) and Figure 2-4 (landscape features and instantaneous changes). Details of the underlying models are presented in the remainder of this chapter.

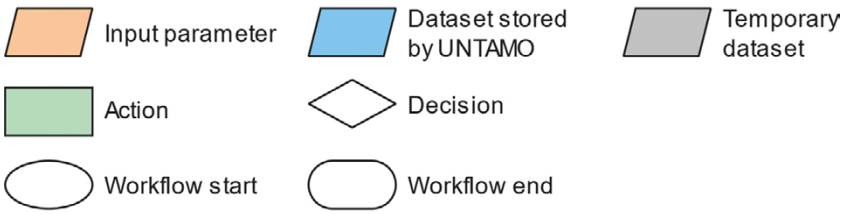

Figure 2-1. *Common legend for all flowcharts.*

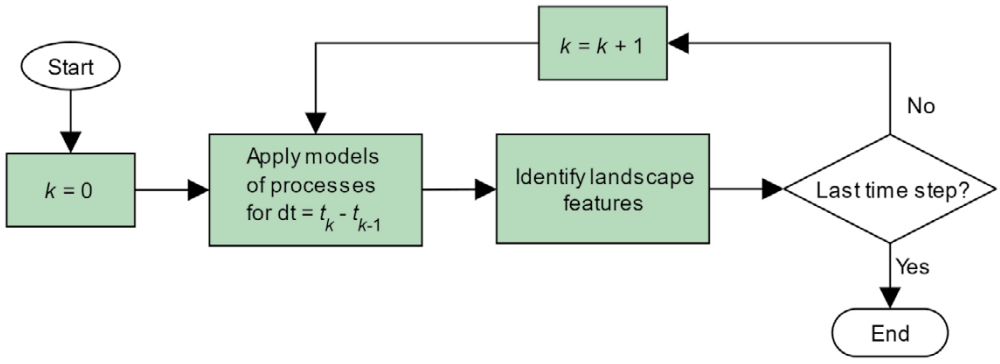

Figure 2-2. *Main time-stepping loop of UNTAMO. The action "Apply models of processes…" is further explained in Figure 2-3. The action "Identify landscape features" is further explained in Figure 2-4.*

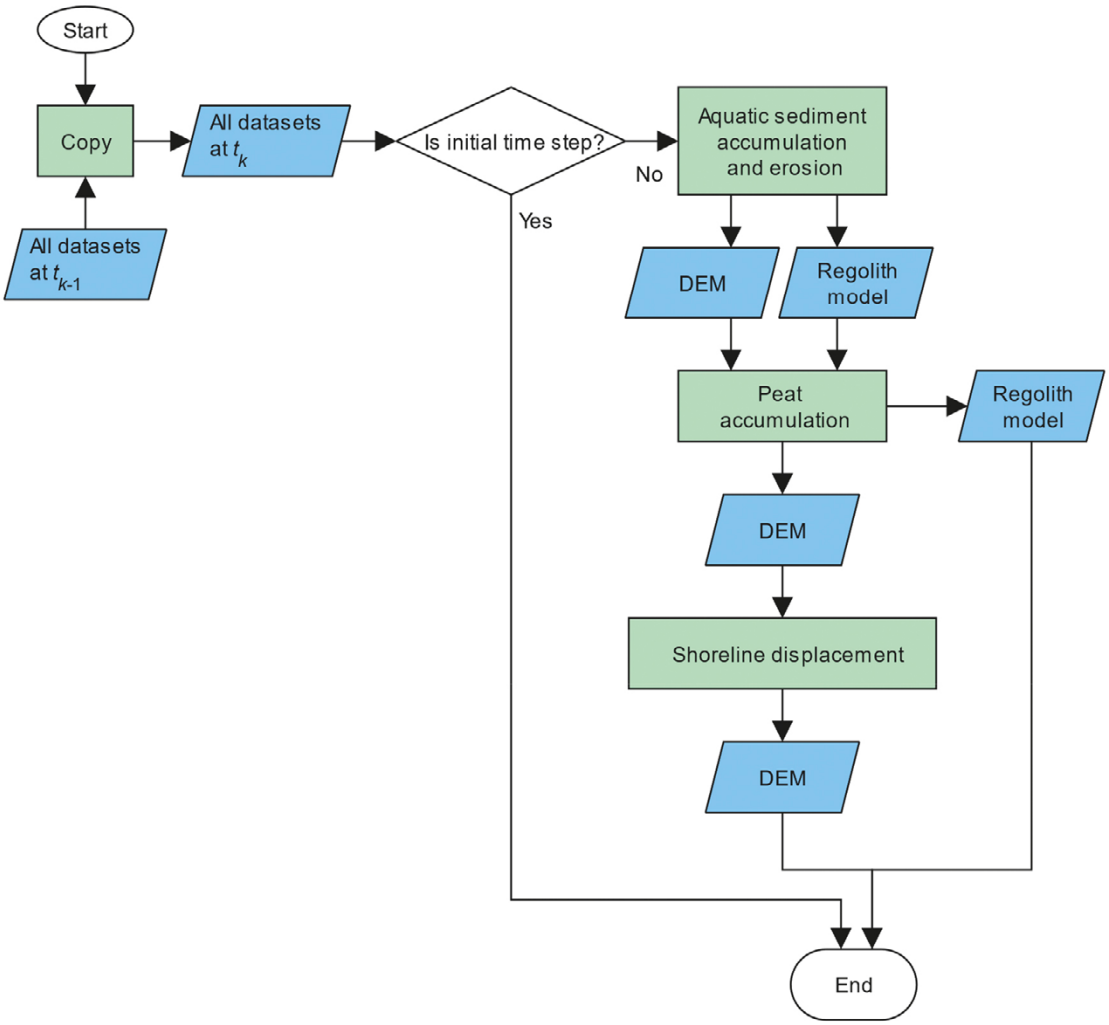

Figure 2-3. *Process models applied for each iteration of the main time-stepping loop. All datasets from the previous time-stepping iteration are copied to the current time step first. In case of the initial time step (k=0), data of the initial condition is copied instead.*

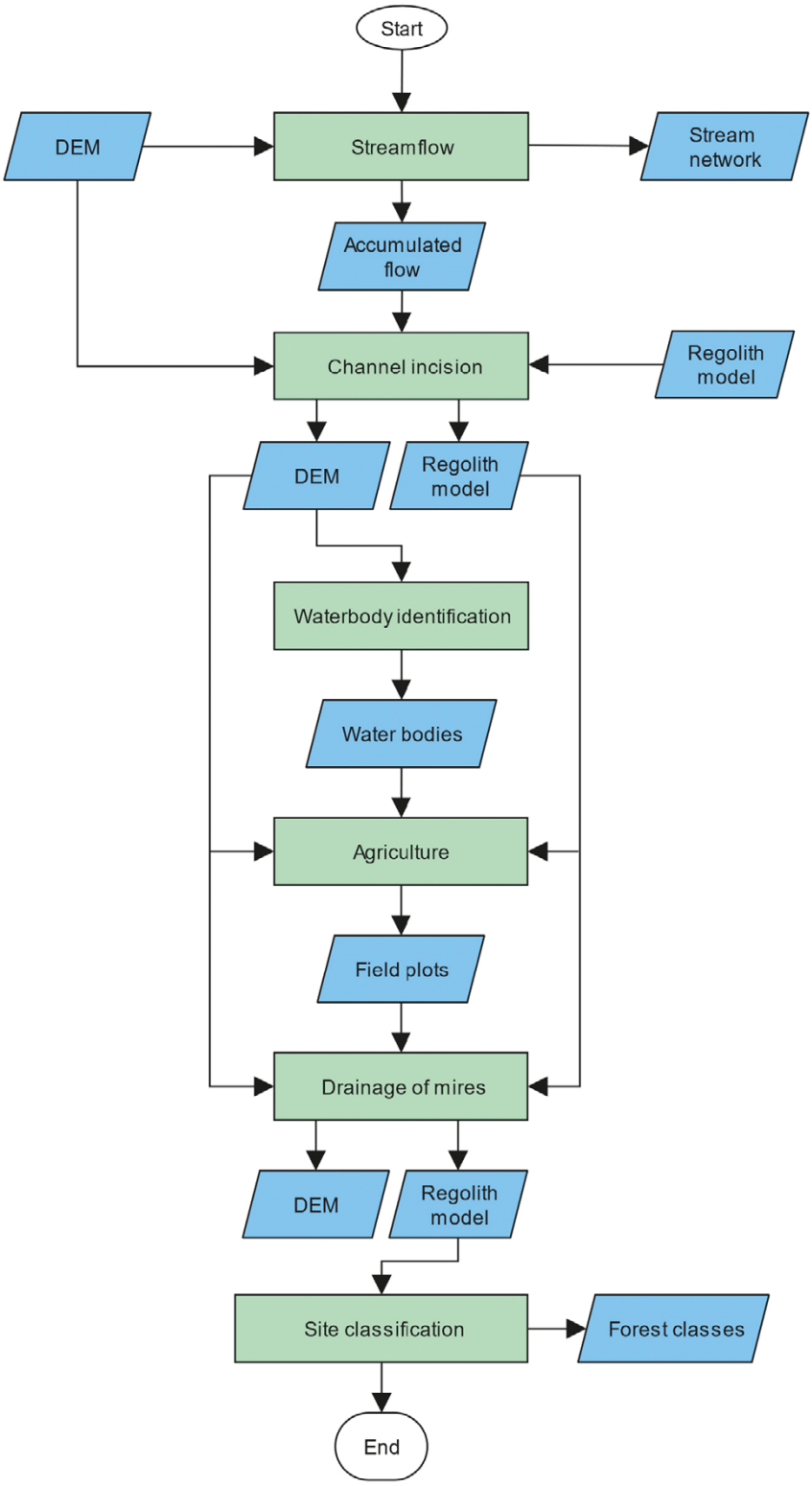

Figure 2-4. *Identification of landscape features and instantaneous landscape changes applied during one iteration of the main time-stepping loop. Please note that while "Channel incision" and "Drainage of mires" are in fact processes, they are assumed to be shorter than the time stepping interval and are applied immediately for simplicity.*

2.1.1 Modelled ecosystems

The landscapes modelled by UNTAMO are summarized in Table 2-1 and Figure 2-5. The description of each landscape and how it is defined is given below. Please note that the description is only brief and references to the appropriate model description sections are given.

2.1.1.1 Sea

Terrain elevation is expressed relative to the sea level in UNTAMO. Therefore, the sea landscape is defined as areas with elevation at or below 0 m above sea level which are also explicitly marked as sea. The sea landscape consists of a littoral zone and open water part. Littoral zones are characterized by dense colonies of vascular plants and are located in shallower parts of the sea (typically with water depth less than 2 m). The remainder of the sea is classified as open water. See Section 2.3.4.1 for more information about sea delineation and Section 2.3.4.4 for information about classification of littoral zones.

Table 2-1. Ecosystems modelled by UNTAMO.

Ecosystem type	Landscape	Landscape sub-type
Aquatic	Sea	Open water Littoral zone (reed)
	Lake	Open water Littoral zone (reed)
	River	-
Terrestrial	Cropland	-
	Forest	Rocky forest Heath forest Grove Mire

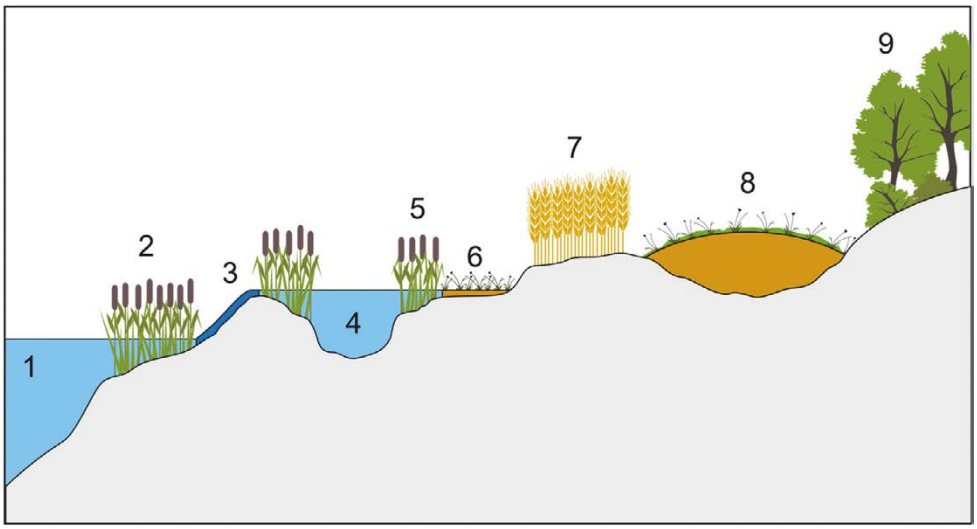

Figure 2-5. *Overview of landscapes handled in UNTAMO, and their parts. 1) Sea open water, 2) sea littoral zone, 3) river, 4) lake open water, 5) lake littoral zone, 6) lake edge mire, 7) cropland, 8) mire (raised bog), 9) forest (all types except mire).*

2.1.1.2 Lake

Sufficiently large depressions in the terrain not identified as sea are assumed to be filled with fresh-water and are classified as lakes. Only parts of the depression with water column deeper than a given limit (30cm by default) are considered lake. Shallower parts are considered to constitute the lake margins and are classified as fen mires (see Sections 2.3.2 and 2.3.4.3).

Lakes are divided into littoral and open water parts. Similarly to the sea, the littoral zone is characterized dense colonies of vascular plants and is located in shallower parts of the lake (typically less than 2 m water depth). The remainder of the lake makes up the open water part. See Section 2.3.4.1 for more information about lake delineation and Section 2.3.4.4 for information about classification of littoral zones.

2.1.1.3 River

Areas with sufficiently large accumulated flow are classified as rivers. See Section 2.3.3 for more information.

2.1.1.4 Cropland

Terrestrial landscapes can be classified as croplands based on soil suitability and the desired density of croplands expressed as fraction of the total terrestrial area. Mires can be drained and converted to croplands. See Section 2.3.6 for more information about conversion of land for agriculture and mire drainage.

2.1.1.5 Forest

Terrestrial areas not classified as cropland are classified as forest. Forest areas with sufficiently thick accumulated peat layer are classified as mire, the remaining areas are classified as either rocky forest, heath forest or grove, depending on soil thickness and soil type.

Peat accumulation occurs in terrain depressions (where lake is not present) and in shallow lake margins and is described in Section 2.3.2. Classification of the remaining forest types is described in Section 2.3.7.

2.1.2 Main drivers of landscape evolution

This section briefly explains the main driver of landscape evolution implemented in UNTAMO. The drivers include shoreline displacement, terrestrialization of shallow sea bays and lakes, mire formation, agriculture and mire drainage. The drivers and their effect on ecosystem succession is shown in Figure 2-6, model details are given in Section 2.3.

2.1.2.1 Shoreline displacement

Shoreline displacement is the effect of continuous advancement of sea shoreline due to post-glacial rebound (also called glacial isostatic adjustment) and the associated eustatic sea level change. During the last glaciation, parts of the Earth's surface have been covered by an ice sheet, up to several kilometres thick during the glacial maximum at around 20 000 years ago. The pressure exerted by the ice at the Earth's crust led to the underlying layer, the mantle, to flow away from the loaded areas. After the ice sheets have retreated, the reversed flow of the mantle back to the de-glaciated areas cause the crust to rise upwards. The process is still ongoing and is expected to take many millennia before the equilibrium state is reached due to the very high viscosity of the mantle. The eustatic sea level change is the change in the global sea level due to changes in the water volume of world's oceans and changes in the volume of ocean basins associated with the post-glacial rebound. The model of shoreline displacement is presented in Section 2.3.2.1.

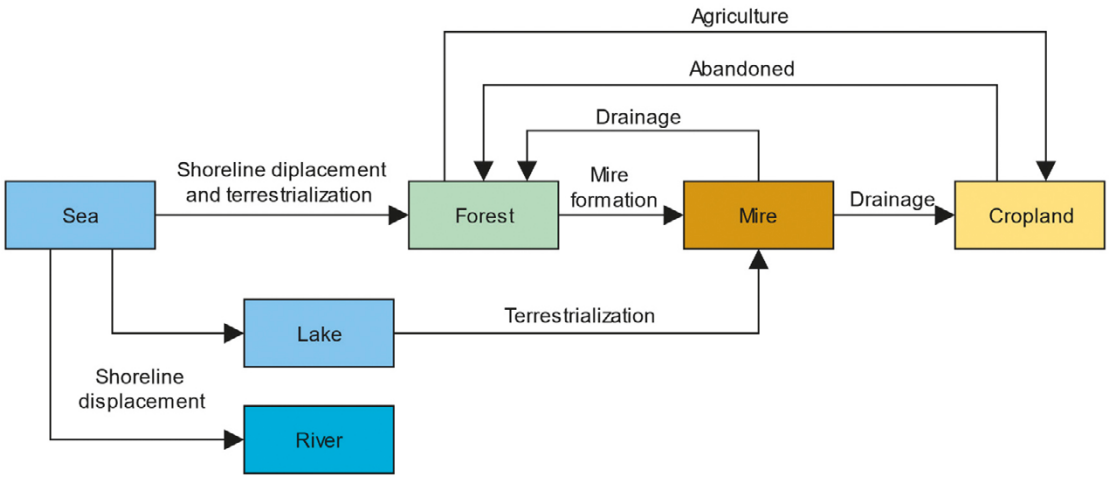

Figure 2-6. *Main lines of succession implemented in UNTAMO.*

2.1.2.2 Terrestrialization of coastal bays and lakes

Terrestrialization refers to continuous colonization of aquatic systems by plants, resulting in conversion from of the aquatic landscape to terrestrial one. Shoreline displacement and sediment accumulation cause coastal regions to become more shallow. Shallow waters are subsequently colonized by aquatic vegetation that accelerates the rate of sediment accumulation as dead plant matter sinks to the bottom. The bay finally becomes isolated form the sea, becoming a lake or a forest. The terrestrialization of a coastal region is illustrated in Figure 2-7, the sediment accumulation module implemented in UNTAMO is described in detail in Section 2.3.1.

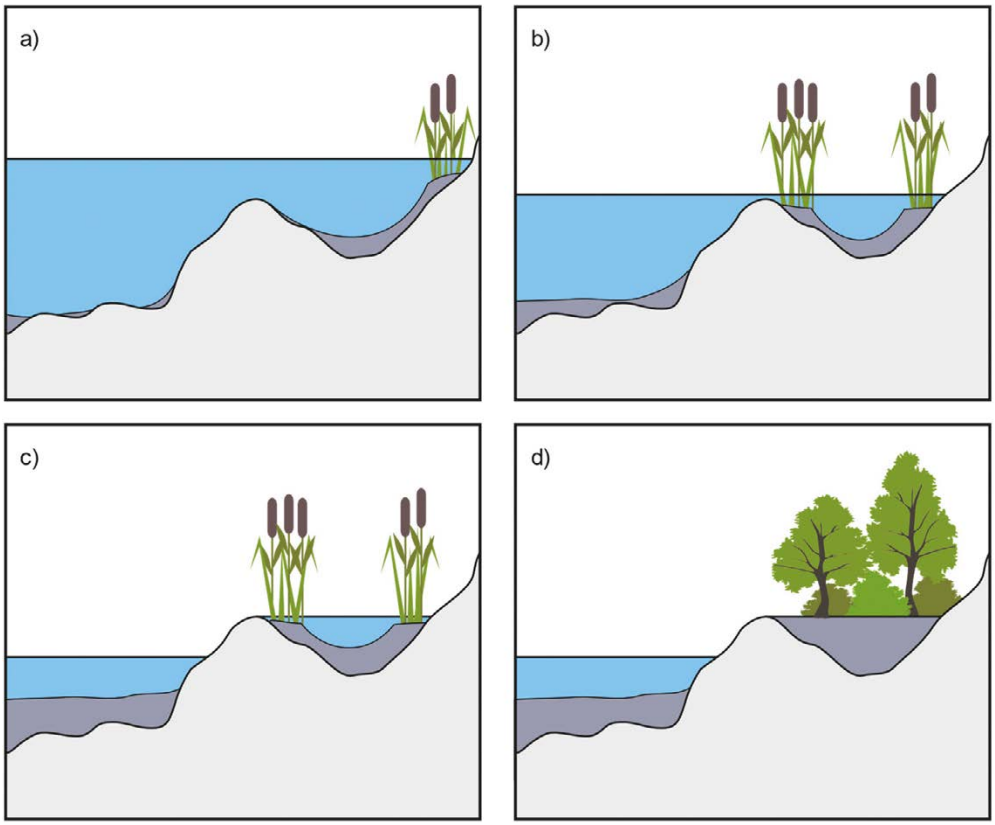

Figure 2-7. *Terrestrialization of shallow coastal regions. a) Organic sediment is accumulated on sea floor (accumulated sediment shown in grey color), b) areas become shallower due to land uplift and continued sedimentation, c) shallow bay is isolated from the sea and becomes lake, d) shallow bay is fully filled by sediment when isolated from the sea and is colonized by plants and trees, eventually developing into a forest.*

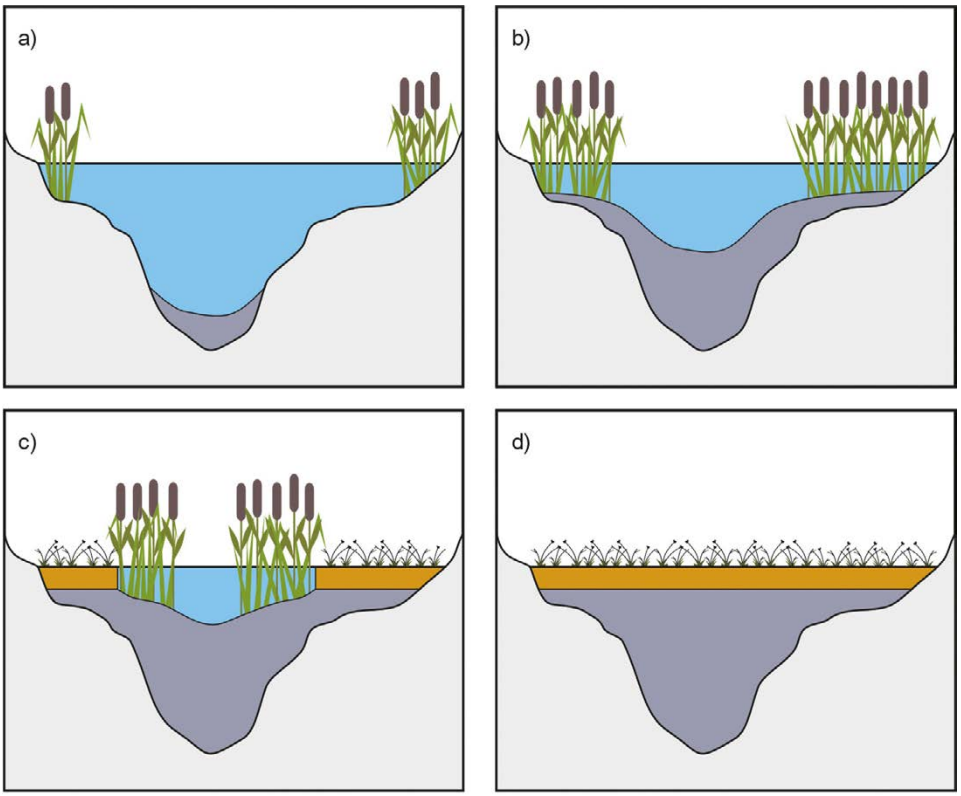

Figure 2-8. *Terrestrialization of a lake. a) Shores of a lake basin are slowly colonized by vegetation, b) lake becomes shallower due to sediment accumulation (organic sediment shown in grey color) in open water and littoral zone, lake becomes overgrown with vegetation, c) part of the lake near shoreline is converted to a mire, d) the lake basin has been filled with organic sediment and a mire develops in its place.*

Sediment accumulation continues in lakes until the lake is eventually fully overgrown. If suitable conditions prevail, the basin may develop into a mire and peat accumulation will continue. The terrestrialization of a lake is illustrated in Figure 2-8, the sediment accumulation module implemented in UNTAMO is described in detail in Section 2.3.1.

2.1.2.3 Mire formation and peat accumulation

Mires are landscapes maintained by a moist local climate and a high groundwater table, where only partially decomposing organic matter accumulates as peat. Mire habitats are dominated by peat forming vegetation. According to soil classification of the Geological Survey of Finland, mires are defined as sites with an at least 30 cm thick peat layer. Mires may form through three main processes:

- Primary mire formation – Growth of mire vegetation directly on fresh soil surface, e.g. after emergence of a site from sea water due to land uplift (Korhola and Tolonen 1996).
- Paludification – Conversion of a forest to a mire ecosystem when the local hydrological conditions shift towards a positive hydrological balance (Huikari 1956, Korhola and Tolonen 1996).
- Terrestrialisation of lakes – Hydroseral succession from open water basin to mire (Korhola and Tolonen 1996). For eutrophic, low, sheltered lakes, terrestrialisation proceeds from bottom to surface, started by sedges, reed and horsetail, and followed by mosses which initiate the height growth of the mire. For ombrotrophic, small lakes, terrestrialisation proceeds from surface to bottom, initiated by floating moss carpets and followed by sedges (Kivinen 1948).

There are different types of mires. Bogs store and release water to and from the surrounding land but are not connected to a system of lakes or streams. Bogs are nutrient poor and generally have a low plant diversity. *Fens* are connected to slow flowing water of small lakes and streams. They are nutrient rich and thus more productive and biologically diverse than bogs.

2.1.2.4 Agriculture

Agriculture refers to the practice of cultivating plants and livestock. Land is used for agricultural production if the soil type and climatic conditions are suitable and if there is a demand for crop or livestock products. Besides the naturally suitable soil types also peat land can be converted into cropland or pasture after drainage.

2.1.2.5 Drainage of mires

Mires can be drained to increase the productivity of peatland forests or to convert the site into a cropland or pasture. Mire drainage involves the creation of ditches to lower the groundwater table. After drainage, the vegetation composition starts changing. Over time, peat forming vegetation disappears and is supplanted by forest species unless the area is used for agriculture. For both types of mire conversion (to forest or to cropland), peat soil becomes compacted and its bulk density increases due to the reduced water content.

2.2 Numerical representation

2.2.1 Model grid

The spatial domain over which the landscape evolution is modelled is represented numerically by a two-dimensional grid in cartesian (projected) coordinate system. The coordinate system should be supported by the QGIS software. It is recommended that the grid has square cells such as 10×10 or 20×20 m. Non-cartesian coordinate systems cannot be used with UNTAMO.

For convenience, the model grid is defined by the initial condition DEM dataset (see Chapter 3) so that the model grid is snapped to the pixels of the DEM dataset.

2.2.2 Time discretization

UNTAMO computes landscape evolution over a series pre-defined time-steps. At the end of each time-stepping iteration, UNTAMO produces data that represents “snapshot” of the state of the landscape at the given time.

The time-stepping interval does not need to be constant and temporal resolution can, for example, be increased where significant changes in the landscape occur (such as transition of a sea bay or a lake from aquatic to terrestrial stage). It is the responsibility of the modeler to define the modelling time steps; UNTAMO does not use automatic adaptive time-stepping. The default time-stepping interval is 500 years.

2.2.3 Conceptual model of regolith

The regolith stratigraphy is represented using a depth-integrated model in which individual layers are stacked on top of each other in fixed order. The thickness of each regolith layer is then represented by a non-negative real value assigned to the model grid cell. If certain layer does not exist in a model grid cell, its thickness is set to zero. The conceptual stratigraphy model is shown in Figure 2-9.

The interpretation of the regolith layers is up to the modeler, but specific layers are required by UNTAMO as listed in Table 2-2 (in the given order).

The peat and organic accumulation layers typically consist of “soft” sediments that are easily eroded. Additional sediment layers, such as mineral layers, can be added if needed but they are not affected by UNTAMO. Soft sediments precede (be located on top of) hard sediments in the layer order as they may be eroded or accumulated at the surface. A layer representing bedrock is also required.

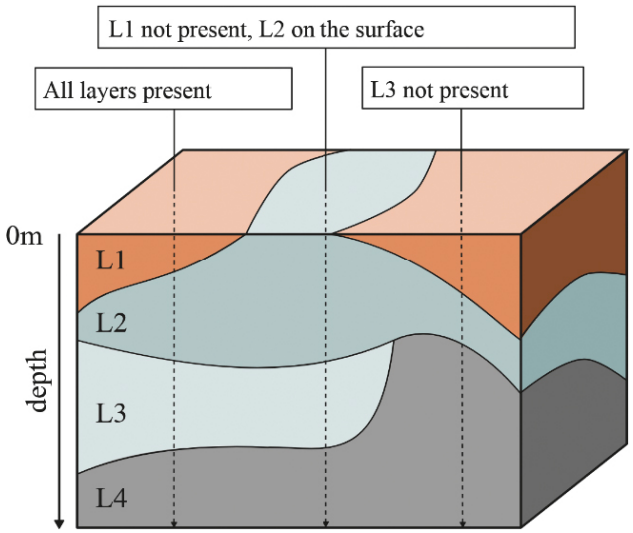

Figure 2-9. *Example of the depth-integrated stratigraphy model with four hypothetical regolith layers L1, L2, L3 and L4.*

Table 2-2. Sediment layers required by UNTAMO.

Regolith layer type	Regolith layer	Description
Soft	Peat	Layer receiving accumulated peat from actively growing mires. This is typically the top-most layer.
	Compacted peat	Layer containing peat after it is compacted due to drainage. Its bulk density will be higher than that of "natural" peat. The compacted layer must be located *directly below the peat layer* in the stratigraphy model.
	Organic accumulation layer(s)	Soil layer or layers that receive accumulated sediment from aquatic accumulation (if aquatic sediment accumulation is in use). Different layers can be used for sediment accumulated during the sea and lake stages.
Hard	Mineral soil layer(s)	Zero or more mineral soil layers. Optional.
	Bedrock	The bedrock layer is required and must be the last layer in the stratigraphy model.

2.2.4 Numerical representation of data

Landscape properties are internally represented as a collection of raster datasets aligned with the model grid so that each pixel represents one model cell. The datasets are stored in GeoTiff format which, in addition to the pixel data, also stores the coordinate system information. Real-valued quantities (terrain elevation, soil thickness, water depth, etc.) are represented using 32-bit floating point data type. Class information (such as landscape type) and object label maps (each pixel stores ID of an object or region) are stored as 32-bit integer rasters. NoData pixels are used to denote missing data or absence of an object or landscape. The input and output dataset are described in more detail in Chapter 3.

2.3 Models of features, events and processes

2.3.1 Aquatic sediment accumulation and resuspension

The aquatic sediment accumulation and resuspension module aims to estimate the amount of sediment that is deposited or eroded (resuspended) from lake or sea bottom over the time frame of the landscape evolution modeling. An important factor for the estimation of the sedimentation rate is the *sediment balance* – the net amount of sediment available for accumulation once sediment that has been resuspended and transported away has been accounted for. The sources of suspended sediment

include biological production in the water column itself (accumulated organic matter produced by aquatic biota, decayed organic matter), resuspension of sediment from the lake or sea bottom and suspended load coming from the upstream catchment. The model consists of a chain of individual sub-modules including, in upstream-to-downstream order:

- Sediment load from upstream catchment.
- Sediment dynamics in lakes (open water).
- Sediment accumulation in littoral zones (lake and sea).
- Sediment dynamics in nearly isolated bays.
- Sediment dynamics in sea (open water).

The chain is composed so that the sediment load output from one sub-module provides sediment input to the downstream modules (Figure 2-10). Sediment transport starts with erosion and transport of terrestrial soil overland, until it eventually reaches the streamflow where it is suspended in the rapidly moving water and transported downstream. In UNTAMO, overland sediment erosion and transport is not modelled directly but may be added in a future update (see Chapter 4). Instead, sediment transport within stream network is modelled using a statistical relationship between the suspended load and upstream catchment properties, described in Section 2.3.1.1. The transported sediment eventually reaches a lake, where water movement slows down causing part of the suspended solid particles to settle to the bottom. The model of sediment dynamics within the open water zone of a lake is described in Section 2.3.1.3. Littoral zones within the lake are treated separately from the open water part; it is assumed that the net sediment flux between the littoral zone and open water is zero. Sediment accumulation in littoral zones is described in Section 2.3.1.2. Eventually, transported sediment will reach the coastal regions, where it may be deposited near the shore (see Section 2.3.1.4) or transported further and deposited in the open sea. The model of the sediment dynamics in the open sea is similar to the sediment dynamics model used for lakes and therefore also described in Section 2.3.1.3.

2.3.1.1 Suspended load from upstream catchment

The statistical relationship between the suspended sediment concentration and stream discharge is commonly known as the *rating curve* and is often expressed in the form of a power law (Syvitski et al. 2000):

$$C_{SS}(Q) = aQ^b \tag{2-1}$$

where Q (m^3/s) is the discharge, a and b are the rate curve coefficients. In UNTAMO, suspended sediment concentration is computed using the upstream contributing area, which is directly related to the discharge as described in Section 2.3.3. If the upstream catchment contains lakes, the catchment area is only computed between the outlet of the upstream lake and the location along the streamflow for which sediment concentration is being estimated. This is because sediment concentration in lake outlets is assumed to be constant (see Section 2.3.1.3) and therefore does not depend on the catchment properties of the upstream lake. This simplification also allows the suspended sediment concentration and suspended load to be computed beforehand, without interaction with the lake sediment dynamics sub-modules. The suspended sediment concentration is therefore given as

$$C_{SS}(A) = aA^b \tag{2-2}$$

where A (ha) is the area of the upstream catchment (from the first upstream lake if such exists). Alternatively, the area be computed only for agricultural land within the upstream catchment and used in the relation. The coefficients a and b are obtained by model calibration using suspended sediment concentration measurements. The equation has been tested by Gunia and Gunia (2022), using water quality data and catchment areas from Southwest Finland, and was found suitable. Suspended sediment concentration can be made constant by setting $b = 0$. Finally, the suspended load Q_S (kg/a) is calculated by multiplying the sediment concentration with discharge

$$Q_S = Q\ aA^b \tag{2-3}$$

The computation of sediment load from upstream catchment is shown in Figure 2-11.

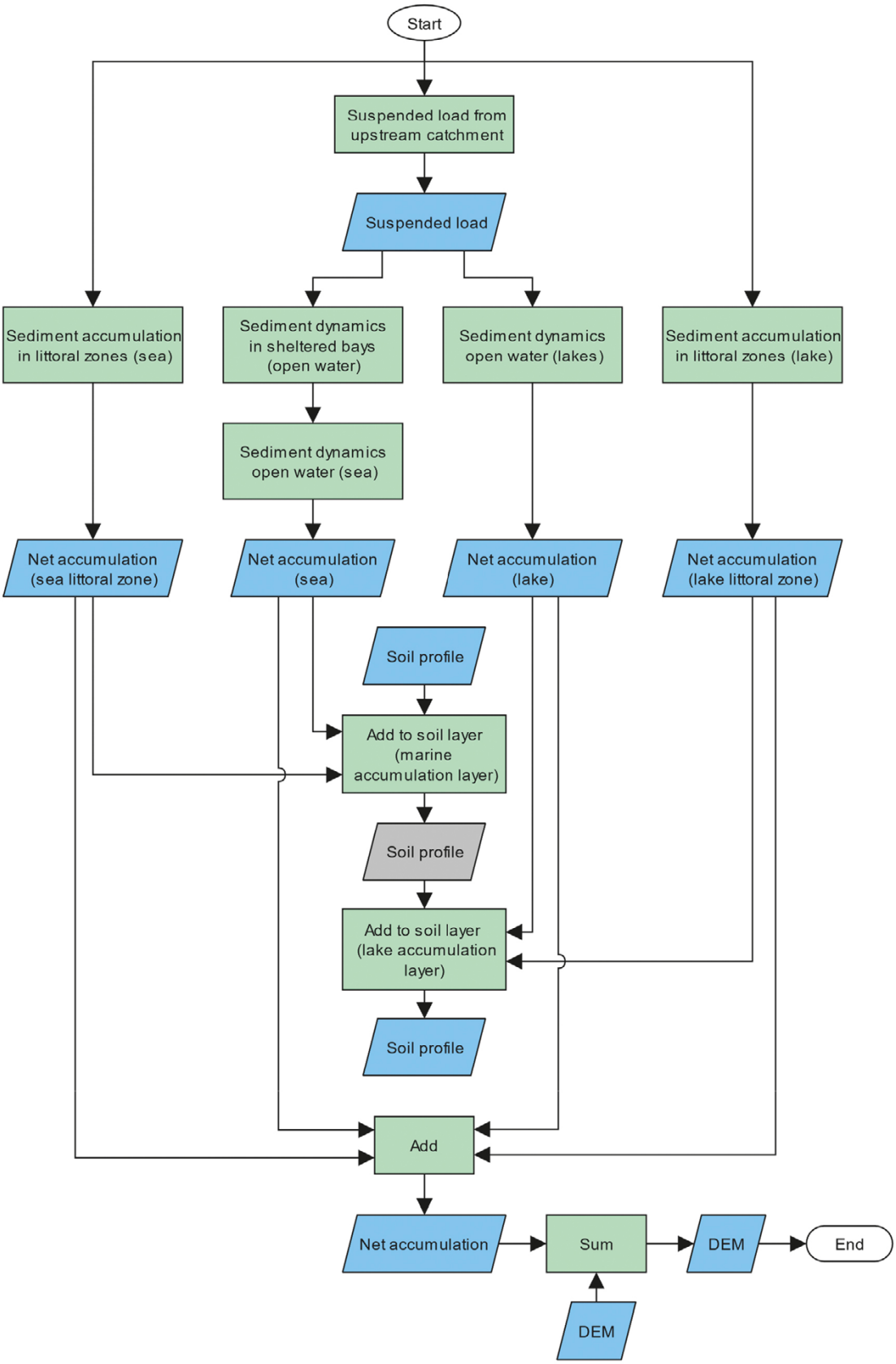

Figure 2-10. *Sediment accumulation and resuspension in aquatic environments. The net accumulated (eroded if accumulation is negative) sediment is added to the DEM and soil profile. Only selected main output datasets are shown in the figure.*

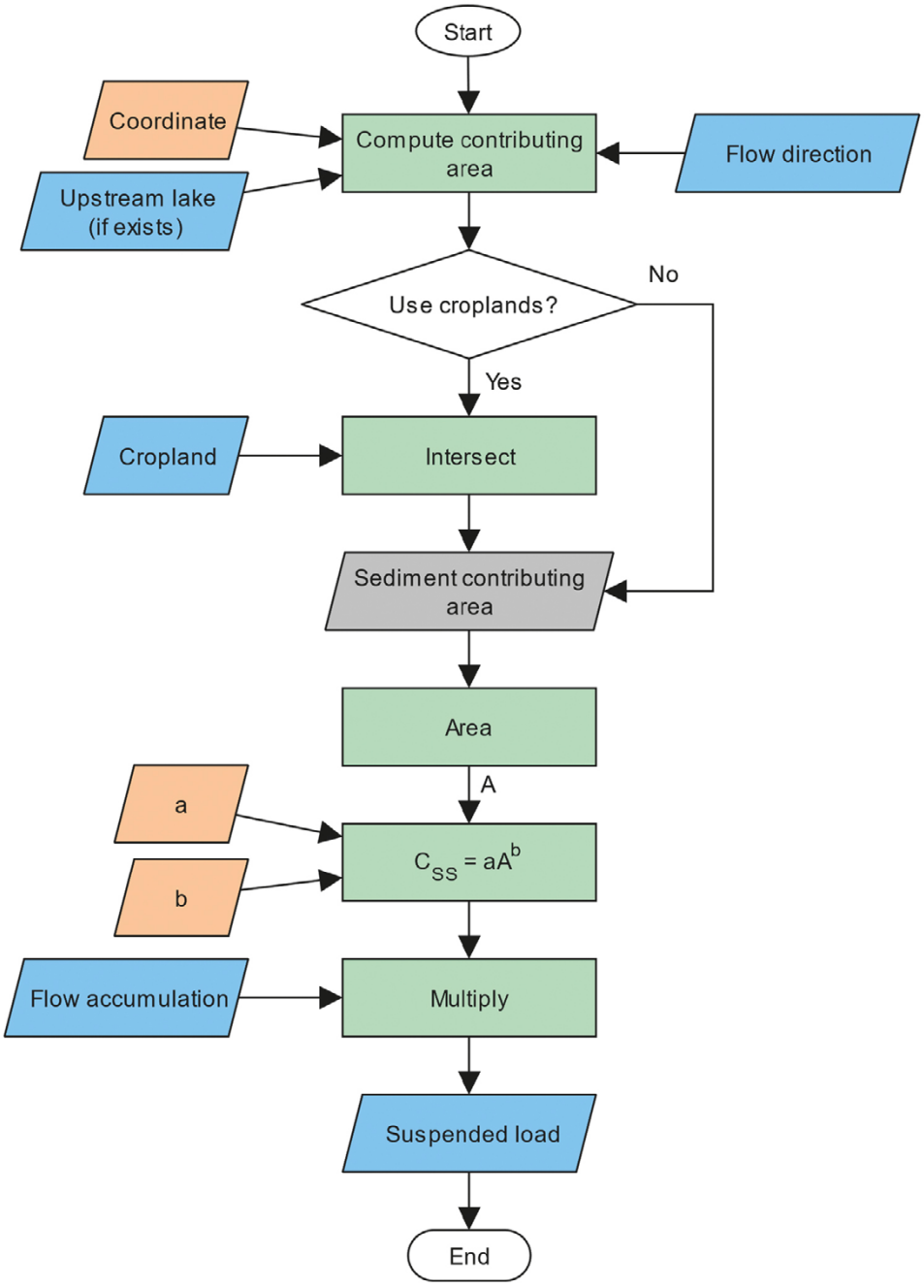

Figure 2-11. *Computation of suspended load for given coordinate from the upstream catchment. Only the contributing area between the coordinate and the first upstream lake (if such exists) is considered.*

2.3.1.2 Sediment accumulation in littoral zones

In UNTAMO, the lake and sea landscapes are divided into the "littoral zone" and "open water", as described in Section 2.3.4.4. Littoral zones are characterized by dense colonies of vascular plants and for the purpose of the sediment accumulation and resuspension modelling it is assumed that the net sediment flux between the littoral and open water zones is zero. Sediment accumulation and resuspension rate in both zones is therefore independent of each other. The assumption is taken due to the lack of available data on water mixing rates between the two zones and on the expectation that water exchange is generally rather limited due to the shallow nature of the littoral zone and that water movement is generally limited by the dense vegetation characteristic of these areas. Littoral zones are treated as accumulation environments, i.e. environments where sediment accumulates continuously. Accumulation environments are further explained in Section 2.3.1.3. Unlike in the open water part, sediment accumulation proceeds at a constant rate ($kg/m^2/a$) in littoral zones.

2.3.1.3 Sediment dynamics in open water

Open water refers to parts of lakes and sea that are not classified as "littoral zones" and are not colonized by dense shoreline vegetation (such as the common reed). Sediment transport in open water is modelled empirically based on the properties of the water body such as water depth and shear stress at the bottom, which are further explained in the sections below. The choice of a simplified empirical model is a practical one: physically based CFD (computational fluid dynamics) models typically represent the transport domain by a network of finite elements or volumes and can accurately model the flow of water and suspended particles in two or three dimensions. However, the complexity of such models and the time needed to execute them makes them unpractical given the rather large spatial domain and exceedingly long modelling time frames handled by UNTAMO. Empirical models, on the other hand, are easier to set up and quick to execute, so they can be readily integrated into the workflow of the terrain and ecosystem modelling. On the negative side, these models usually contain parameters that cannot be derived directly from physical properties of the materials involved but must be obtained through calibration to observed data.

For modelling sediment accumulation and resuspension (the suspension and redistribution of previously deposited particles), open water is first classified into *erosion*, *transport,* and *accumulation* environments, similarly to the approach used in Brydsten and Strömgren (2013). The environments are defined as

- Erosion environments – characterized by frequent sediment resuspension such that sediment particles do not have time to settle before they are resuspended again. Resuspended particles are transported to calmer waters (accumulation environments) where they eventually settle.
- Accumulation environments – characterized by reduced water movement that allows suspended sediment particles to settle continuously (or with infrequent resuspension between accumulation periods).
- Transport environments – assigned to the remaining areas. The net sediment accumulation rate is assumed to be zero in the transport environments.

Detachment of sediment particles from the bottom and subsequent suspension in water is driven by stress exerted on the bottom by moving water. Wind-induced waves at the surface generate circular motion in the water below as part of the wave energy is dissipated into the water column. Water currents near the bottom may also significantly contribute to the shear stress and consequent resuspension of particles.

The concept of sediment transport from erosion to accumulation environments is shown in Figure 2-12. It should however be noted that the sediment accumulation and resuspension module is not a physical model and particle movement is not explicitly tracked. Instead, the model relies on long-term sediment accumulation and erosion rates that are obtained through model calibration.

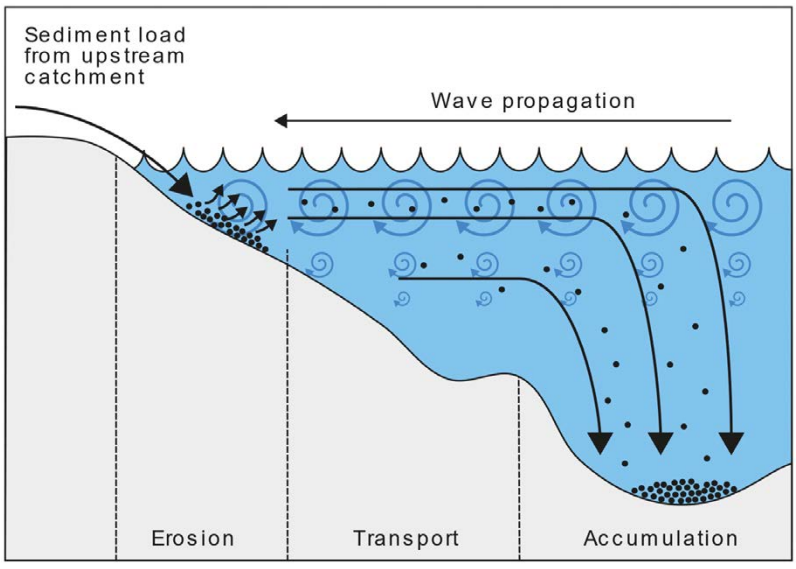

Figure 2-12. *Classification of open-water areas of the sea into erosion, transport and accumulation environments based on wind-induced wave action. Suspended sediment is transported from the upstream catchment into the water body and transported, together with resuspended sediment, further into accumulation environments where it gradually settles to the bottom.*

The net annual sediment balance ΔS (kg/a) in the aquatic system is given by the balance equation

$$\begin{aligned} \Delta S &= S_a - S_e \\ S_a &= p_a A_a + Q_{S,in} - Q_{S,out} \\ S_e &= r_e A_e \end{aligned} \quad (2\text{-}4)$$

where S_a (kg/a) is the gross sedimentation rate in accumulation environments and S_e (kg/a) is the gross erosion rate in erosion environments. p_a (kg/m^2/a) is the calibrated unit 'sediment production rate' accounting for organic material that is the result of biological production within the water column and suspended sediment carried from elsewhere within the system, r_e (kg/m^2/a) is the unit sediment erosion rate in erosion environments, $Q_{S,in}$ (kg/a) is the suspended load from upstream catchment and $Q_{S,out}$ (kg/a) is the suspended load out from the aquatic system. A_a and A_e (m^2) is the area of the accumulation and erosion environments. Therefore, suspended sediment is eventually accumulated in the accumulation environments or leaves the system (via the $Q_{S,out}$ term). As can be seen from Equation 2-4, in the current model implementation of the model the amount of suspended sediment and consequently the gross accumulation rate S_a is not dependent on the erosion rate S_e. While this approach was used in the RLDM (Brydsten and Strömgren 2013), the methodology has been deemed difficult to justify without tracking the particle movement, an addition that would significantly complicate model calibration. The area of erosion environments and the gross erosion rate also depends on how much shoreline is included in the model domain as erosion is assumed to predominantly occur in shallow waters near the shore.

The total mass of the sediment to be accumulated in an accumulation environment is given by $s_{tot} = S_a^t$. To distribute the sediment over the area of the accumulation environment, several approaches are possible. The simplest way is to distribute sediment evenly with a constant thickness over the accumulation area where the sediment thickness given by $\Delta z_{S,a} = (S_{tot})/(A_a \rho_a)$, where t (a) is the accumulation period and ρ_a (kg/m^3) is the accumulated sediment bulk density. This however will likely lead to unrealistic staircase-like artefacts created in the DEM which are likely to cause problems in subsequent modelling. To avoid this, UNTAMO generates a hypothetical surface that is thought of as the sediment accumulation limit – a surface to which the basin bottom would eventually converge given sufficient sediment input. This hypothetical surface is an assumption made in the model and it is not based on previous studies examining sedimentation in accumulation environments. The limit surface is computed iteratively by first smoothing the original surface with a Gaussian filter, then taking the maximum elevation of the original and smoothed surface at each pixel. The process is repeated with the radius of the Gaussian filter halved until convergence. Therefore, the smoothness of the limit surface is controlled by the choice of the initial smoothing filter radius, for which a representative value can be selected by expert judgement.

The final surface is then calculated as a linear combination of the basin bottom and the accumulation limit surface such that the deposited volume is equal to $(S_a t)/\rho_a$. The thickness of the accumulated sediment is therefore given by

$$\begin{aligned} \Delta z_{S,a} &= (z_{lim} - z) k_a \\ k_a &= \frac{S_a t}{\rho_a} \frac{1}{V_{lim}} \end{aligned} \quad (2\text{-}5)$$

where k_a (-) is the basin "fill fraction" and V_{lim} (m^3) is the volume between the accumulation limiting surface and the basin bottom. An example of the accumulated sediment thickness calculation is shown in Figure 2-13.

Sediment erosion in erosion environments is applied using the same algorithm as sediment accumulation using an inverted DEM. The same erosion rate is applied for all sediment layers regardless of their grain size. Erodible layers can however be specified so that only those sediment layers can be removed; the bedrock layer is never eroded in any case. The sediment accumulation and erosion algorithm is shown in Figure 2-14.

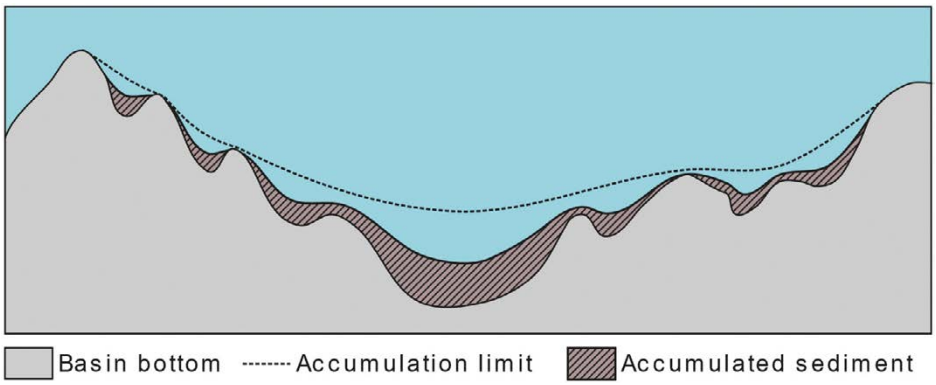

Figure 2-13. *Accumulated sediment thickness computed as a fraction of the volume between the accumulation limit surface (dashed line) and the basin bottom. The accumulation fraction is roughly 0.5 in this figure.*

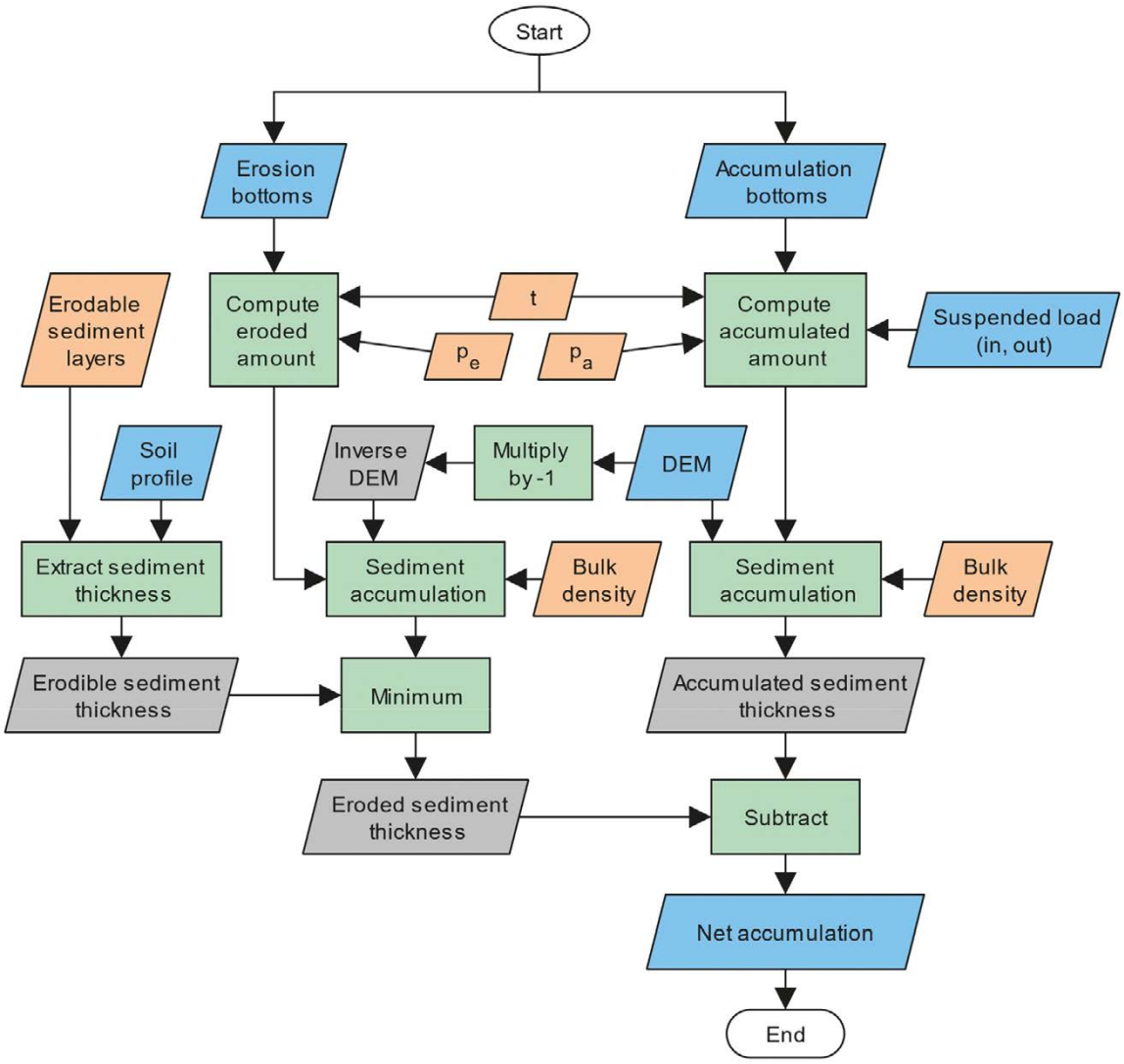

Figure 2-14. *Sediment accumulation and resuspension in marine and freshwater environments. The net accumulated (eroded if accumulation is negative) sediment is added to the DEM and soil profile. Only selected main output datasets are shown in the figure.*

The approach for classifying accumulation and erosion bottoms differs for lakes and coastal regions. Sediment dynamics in coastal regions are described in Sections 2.3.1.4 and 2.3.1.5, sediment dynamics in lakes are described in Section 2.3.1.6.

2.3.1.4 Identifying sheltered bays

Marine bays which only have a narrow connection to the open sea form a special case. Because of the limited water exchange with the remaining parts of the sea, significant portion of the sediment that is transported into the bay is likely going to be deposited within the bay rather than redistributed in the entire coastal region. For this reason, UNTAMO includes an option to automatically detect such sheltered coastal bays using the geometry of the coastline. The criteria for classifying a bay as sheltered is

- The area of the bay must be sufficiently large
- The width of the strait connecting the bay and the open sea must be below given limit

Due to the lack of more detailed information, the sediment balance in a sheltered bay is handled in the same way as for lakes (Section 2.3.1.6). The suspended sediment concentration in the flux from the bay into the open sea is therefore assumed to be constant (with concentration typically being lower than concentration in the influx from upstream) and the discharge out of the bay is set equal to the discharge from the upstream catchment. The classification of accumulation and erosion environments is the same as for the open sea (Section 2.3.1.5). Example of a sheltered bay identification is shown in Figure 2-15.

2.3.1.5 Sediment dynamics in marine waters

The main driving force behind particle resuspension is the movement of water near the bottom and consequently the stress exerted by the moving water layer. Wind-induced waves on the water surface cause elliptical orbital motion on the bottom as part of the energy of the propagating wave is dissipated into the water column. To identify accumulation and erosion environments, wave parameters including the significant wave height H_s (m), period T_s (s) and length L_s (m) are estimated using the SMB method presented in Coastal Engineering Research Center (1984). Inputs to the Sverdrup-Munk-Bretschneider method (SMB) equation are effective fetch (m), wind speed (m/s), duration (h) and water depth (m).

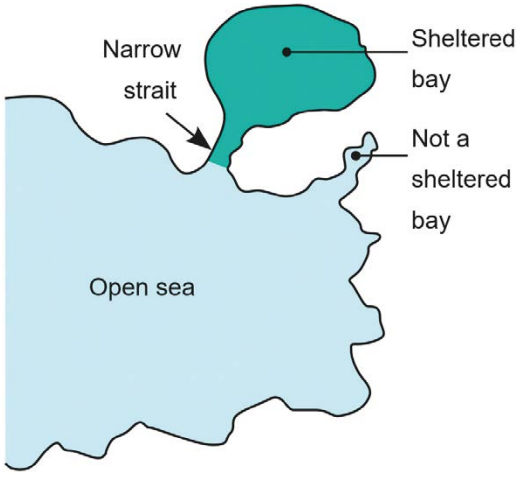

Figure 2-15. *Example of sheltered bay classification.*

The shear stress τ (N/m) exerted on the bottom is then calculated from wave parameters using relationship given by Komar and Miller (1972)

$$\tau = f_w \rho \frac{u_m^2}{2} \tag{2-6}$$

where f_w is the friction factor caused by waves, ρ is water density and u_m is the maximum velocity at the bottom, calculated as

$$u_m = \frac{\pi H}{T_s \sinh\left(\frac{2\pi h}{L_s}\right)}. \tag{2-7}$$

Here H (m) denotes the mean wave height, set to $H = 0.626 H_s$ (Coastal Engineering Research Center 1984) and h (m) is the water depth. The shear stress is then compared to a limiting shear stress needed for resuspension τ_R so that if $\tau \geq \tau_R$, sediment resuspension from the bottom takes place. The τ_R parameter can be obtained through parameter calibration or calculated from typical grain size of the to-be-eroded sediment.

From the definition of accumulation environments, we are looking for environments that experience no or infrequent sediment resuspension so that sediment particles are allowed to settle for most of the time. More specifically, accumulation environments are areas where $\tau < \tau_R$ even during severe weather events. The wind speed and duration for these events are given using the SDM.Sea.AccumWind.Speed and SDM.Sea.AccumWind.Duration parameters, the corresponding shear stress at the bottom will be denoted τ_A. The limiting wind speed and duration can be derived from historical wind observation data and Equation 2-6 by taking observed wind speeds, sustained over given time window, that yield the highest shear stress.

Erosion environments, on the other hand, are areas that experience continuous or frequent sediment resuspension. Therefore, we are looking for areas where $\tau \geq \tau_R$ most of the time. The wind speed and duration for these events are given using the SDM.Sea.ErosionWind.Speed and SDM.Sea. ErosionWind.Duration parameters, the corresponding shear stress at the bottom will be denoted τ_E. The parameters can be derived from historical wind observation data and Equation 2-6 by taking observed wind speeds, sustained over given time window, that yield the highest shear stress and that occur frequently (for example at least once a month or weekly). Therefore, these conditions (or stronger) are expected to prevail and if they lead to sediment resuspension, the area will experience continuous sediment erosion.

Water currents near the bottom may also significantly contribute to the shear stress and consequent resuspension of particles. However, modelling water flow with a computational flow dynamics (CFD) model is deemed impractical. A simpler approach is taken instead where the topography of the sea bottom is used as an indicator of reduced or increased shear stress. This is achieved by computing the local mean elevation difference of a point on the sea bottom and its surroundings. The elevation difference, denoted Δz (m), is computed by taking the elevation difference of the point in question and the average elevation at given radius (spatial scale) around the point. Areas where $\Delta z < \Delta z_E$ are local maxima in the sea bottom that are assumed to experience sediment erosion regardless of the computed wave-induced shear stress. Similarly, areas where $\Delta z > \Delta z_A$ are local minima that are assumed to be sufficiently protected from both the wave action and water currents, allowing sediment particles to settle. The parameters Δz_E and Δz_A are given by the user and by default the elevation difference is not used (therefore by default $\Delta z_E = -\infty$, $\Delta z_A = \infty$).

To summarize:

- For $\tau_A < \tau_R$ or $\Delta z > \Delta z_A$ area is classified as accumulation environment.
- For $\tau_E \geq \tau_R$ or $\Delta z < \Delta z_E$ area is classified as erosion environment.
- Otherwise area is classified as transport environment.

The fetch length required for the calculation of the wave height and period is computed for the sea and is averaged over all directions from which the wind is expected to blow. The range of directions from which wind may blow can be set using the SDM.Sea.AccumWind.MinDir and SDM.Sea.AccumWind.MaxDir parameters for the for accumulation-limiting winds and the SDM.Sea.ErosionWind.MinDir and SDM.Sea.ErosionWind.MaxDir parameters for the erosion-limiting winds. The maximum fetch length can also be explicitly given using the SDM.Sea.MaxFetch parameter. This can be useful for model domains that are not large enough to contain enough shoreline for UNTAMO to calculate the fetch length properly. The maximum fetch length can be given separately for each of the 8 ordinal directions (N, NE, E, SE, S, SW, W, NW) and is linearly interpolated for other directions, thus representing a coarse approximation of the shoreline in a 360-degree circle. The principle of the maximum fetch length approximation is shown in Figure 2-16. In the current version the approximation is static and cannot change with time. An example of the bottom classification is shown in Figure 2-17, the complete algorithm is illustrated in Figure 2-18.

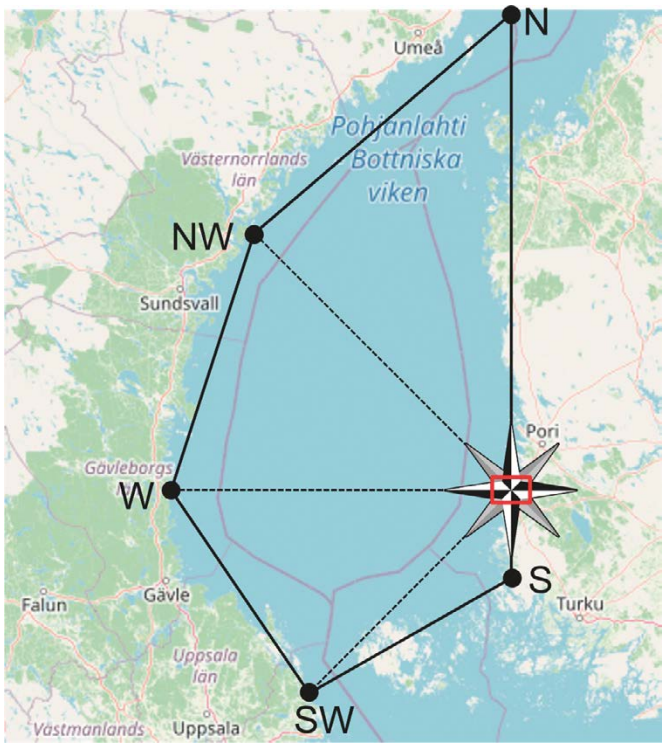

Figure 2-16. *Maximum fetch approximation for a model area (shown as red box) that is too small to contain the entire marine basin (Gulf of Bothnia). Background map from OpenStreetMap (www.openstreetmap.com).*

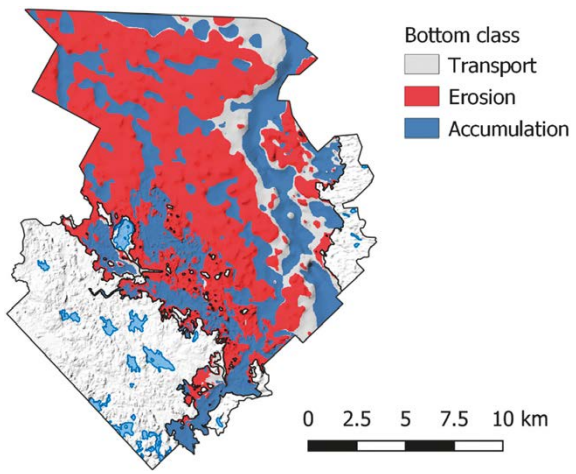

Figure 2-17. *Example marine bottom classification for the Forsmark disposal site, Sweden.*

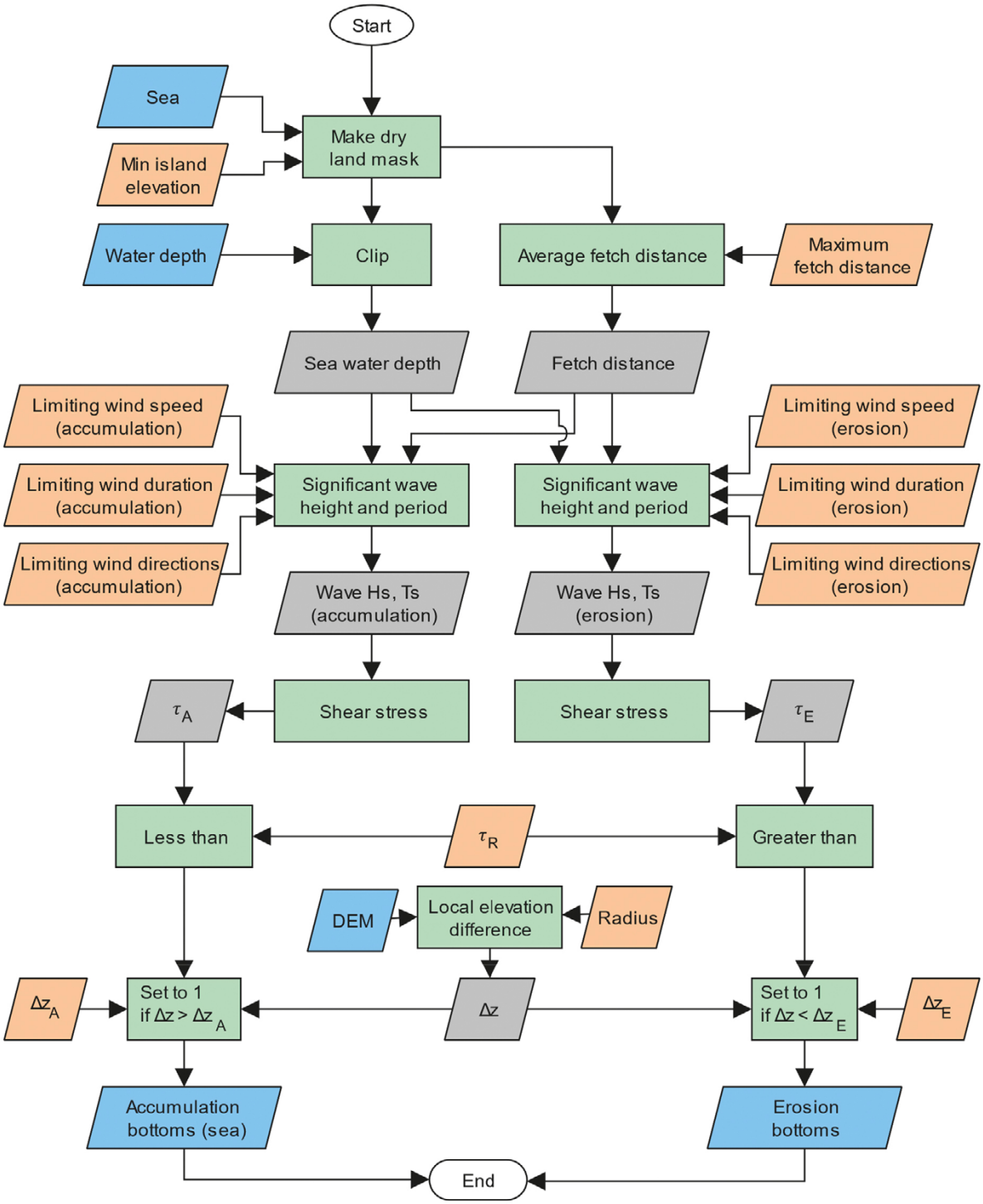

Figure 2-18. *Classification of open-water marine areas into erosion, transport and accumulation environments.*

After accumulation and erosion environments are identified, the model proceeds with sediment accumulation and removal. The marine region is first divided into sheltered bays and open sea (if sheltered bays are in use, see Section 2.3.1.4), each representing separate accumulation zone. The gross sediment accumulation and erosion rates S_a and S_e (Equation 2-4) are computed for each zone separately and the sediment accumulation and erosion algorithm proceeds as described in Section 2.3.1.3. It is not feasible for the current model to estimate the suspended sediment flux to and from the open sea. Therefore, it is assumed that the time-averaged net sediment flux over the boundary separating the accumulation/erosion environments and the open sea is zero and the suspended load term $Q_{S,in}$ in Equation 2-4 only includes suspended sediment load from an upstream catchment. The load out of the system, $Q_{S,out}$, is

therefore assumed to be zero. This assumption is expected to be acceptable if the model domain is large enough to include sufficient area of open sea. More specifically, the water column cross-section of the open sea at the model domain boundary should be large enough so that the net water flux though the boundary, averaged over the duration of the modelling time step, can be assumed to be insignificant.

2.3.1.6 Sediment dynamics in lakes

For lakes, the classification of accumulation environments is simplified and is only based on water depth. This is because good information on lake bathymetry has not been available in areas for which the software has been developed. Additionally, wind data may significantly vary locally based on the surrounding topography, affecting the shear stress computation. Therefore, UNTAMO classifies lake open water (i.e. areas not classified as littoral zones) as either an accumulation environment, if water depth is larger than the given limit, or a transport environment. Erosion environments are not applied in lakes as wave action is much weaker due to the limited fetch. The classification of lakes as accumulation or transport environments is shown in Figure 2-19.

2.3.2 Mire formation and peat accumulation

Mire formation processes in UNTAMO include formation of fen mires near lake shorelines and the development of raised bogs. In UNTAMO, fen mires are located in topographic depressions that contain a lake. Parts of the depression that are too shallow to be considered a lake (the Lake. MinimumWaterColumnDepth parameter) are classified as lake-edge fens. They are typically small, limited initially to a narrow strip around the lake edge. For this reason, peat accumulation is not modelled as a function of time but it is assumed, for simplicity, that the time stepping interval is large enough for the mire to develop. As a result, the shallow area is filled with peat within a single time step during the "landscape feature" calculation phase (see Figure 2-2). The peat is accumulated up to the lake threshold elevation as described in Section 2.3.4.3). It should be noted that the area may continue developing into a raised bog if suitable conditions prevail.

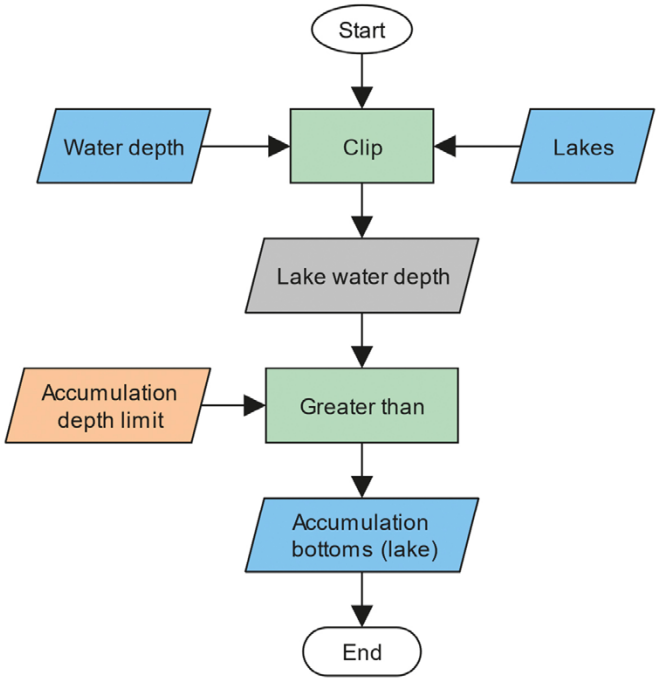

Figure 2-19. *Classification of lake bottoms into transport and accumulation environments.*

Raised bogs, on the other hand, range in size. The largest mires develop over thousands of years and the peat column may reach over 10 meters (Tolonen 1977). UNTAMO does not contain a sufficiently accurate and robust model of subsurface hydrology to compute the depth of the groundwater table. Instead, all terrain depressions that are large enough (but below the lake classification limit) are considered as potential locations where peat bogs may develop. To identify the depressions, the peat layer is first removed from the DEM and the resulting DEM is filled up to the threshold of each depression. The difference between the two DEM datasets then defines the depth of the depression and pixels for which the depth is larger than given limit (Peat.MinSinkDepth parameter) are taken as the starting locations of mire formation. The entire process is illustrated in Figure 2-20.

The development of raised bogs and accumulation of organic sediment from decaying plants is calculated using a semi-empirical model by Clymo (1984). In the model, the peat bog is composed of two layers: on the surface, an aerobic layer several dozen centimeters thick, called the acrotelm, is found in which peat-producing plants grow. Underneath lies a usually much thicker layer called catotelm where anaerobic conditions prevail. The boundary between the two layers is defined by the location of the groundwater table in the peat bog. Dead plant matter passing from acrotelm to catotelm is subject to slow anaerobic decay within the catotelm column. An equilibrium state is eventually reached when the rate of production in the acrotelm layer is equal to the rate of decay in the expanding catotelm layer. Once at the equilibrium state the mire effectively ceases to grow. The concept of the two distinct layers and their role in peat bog development is shown in Figure 2-21. It is worth noting that other factors such as seasonal droughts, which may cause irreparable damage to the mire vegetation, may factor into the ability of mires to grow as well. These factors are not considered by the model.

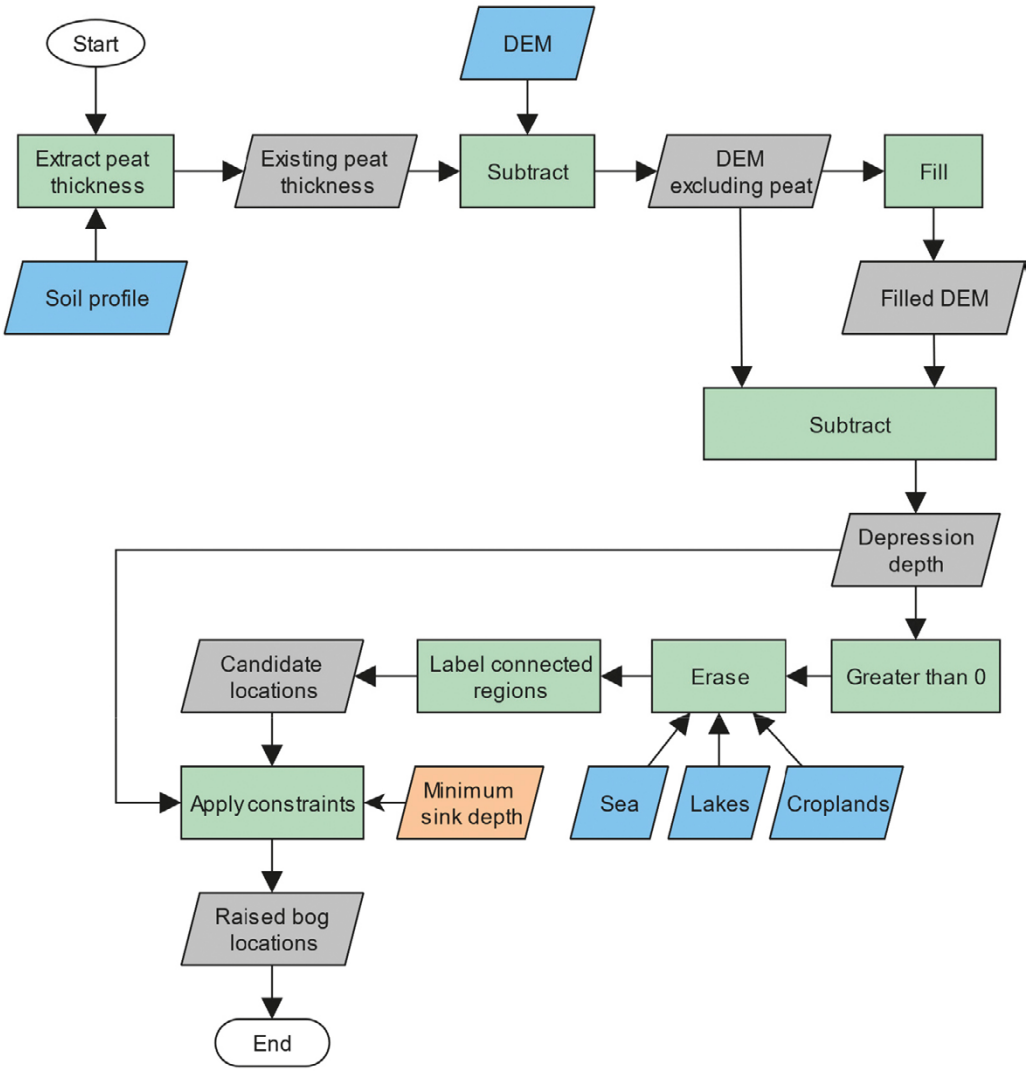

Figure 2-20. *Locating raised bogs from DEM.*

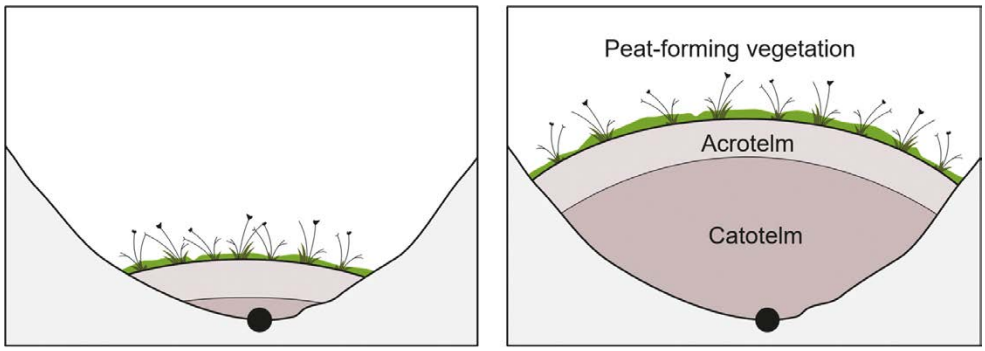

Figure 2-21. *Two-layer structure and development of a raised peat bog. In its early stages (left), the development of the peat bog is dominated by production of organic matter in the surface layer (acrotelm). As the decaying matter passes into the underlying layer (catotelm), the total decay rate in the entire acrotelm eventually balances out the rate of production in acrotelm and the peat bog reaches its asymptotic mass limit (right). The origin of the bog formation is shown with a black dot.*

Mathematically, for small hydrostatic pressure gradients the peat mass can be treated as a porous medium to which Darcy's law applies. The specific discharge U for a circular raised bog can be estimated using

$$\frac{U}{k} = \frac{2H^2}{2Rl - l^2} = \frac{H_m^2}{R^2} \tag{2-8}$$

where H is the peat thickness (m), H_m is the peat thickness at the centre of the bog (m), R is the radius of the bog (m), l is the distance from the perimeter (m), and k is the hydraulic conductivity of the peat formation (m/y). U is the specific discharge from the peat bog ($m^3/m^2/y$). The specific discharge can also be estimated using a water balance where discharge is approximated as the precipitation falling on the bog minus the losses to evapotranspiration, losses to bedrock and the change in the water storage in the bog.

The model to estimate the peat thickness is assumed to be a function of both the distance from the axis point and of time, $H(x,t)$. For a symmetric bog the peat thickness can then be estimated as:

$$H(x,t) = \sqrt{\left(\frac{p_c}{\alpha_c \rho_c}(1 - e^{-\alpha_c t})\right)^2 - \left(\frac{U}{k}\right)x^2} \tag{2-9}$$

where, x is the distance from the axis point (m), p_c the rate of matter passing to catotelm ($kg/m^2/y$, in dry matter), a_c the peat decay rate in the catotelm (y-1), and p_c the dry bulk density of peat (kg/m^3). Equation 2-9 gives a hemispherical bog on a theoretical plane. In reality, however, the border of the bog can be as complex as the surrounding landforms. As explained in detail in Clymo (1984, pp 644–645), the surface elevation of the bog is given by Equation 2-9 and the elevation of the theoretical plane (taken to be the elevation of the origin of the peat bog growth) where the theoretical peat surface is above the actual terrain elevation. Therefore, areas where the surrounding landscape rises above the theoretical peat bog surface are not treated as peat bogs.

From Equation 2-9 it can be seen that the first term on the right side regulates only the maximum peat thickness (i.e. thickness at the axis point), H_m, and the second term the extent (curvature of the surface profile). Thus, the lateral extent of the bog depends here only on the ratio of the water balance and the hydraulic conductivity of the peat (and the subsoil topography), and the maximum thickness depends on the balance of between production and decay of the peat as expressed in:

$$H_m(t) = \frac{p_c}{\alpha_c \rho_c}(1 - e^{-\alpha_c t}) \tag{2-10}$$

The age of each bog is tracked by UNTAMO and the peat thickness as a function of age and horizontal distance from the origin is given by Equation 2-9. The peat accumulated at any time step is then the difference between the peat thickness given by the model and the thickness of existing peat. The peat accumulation algorithm is shown in Figure 2-22.

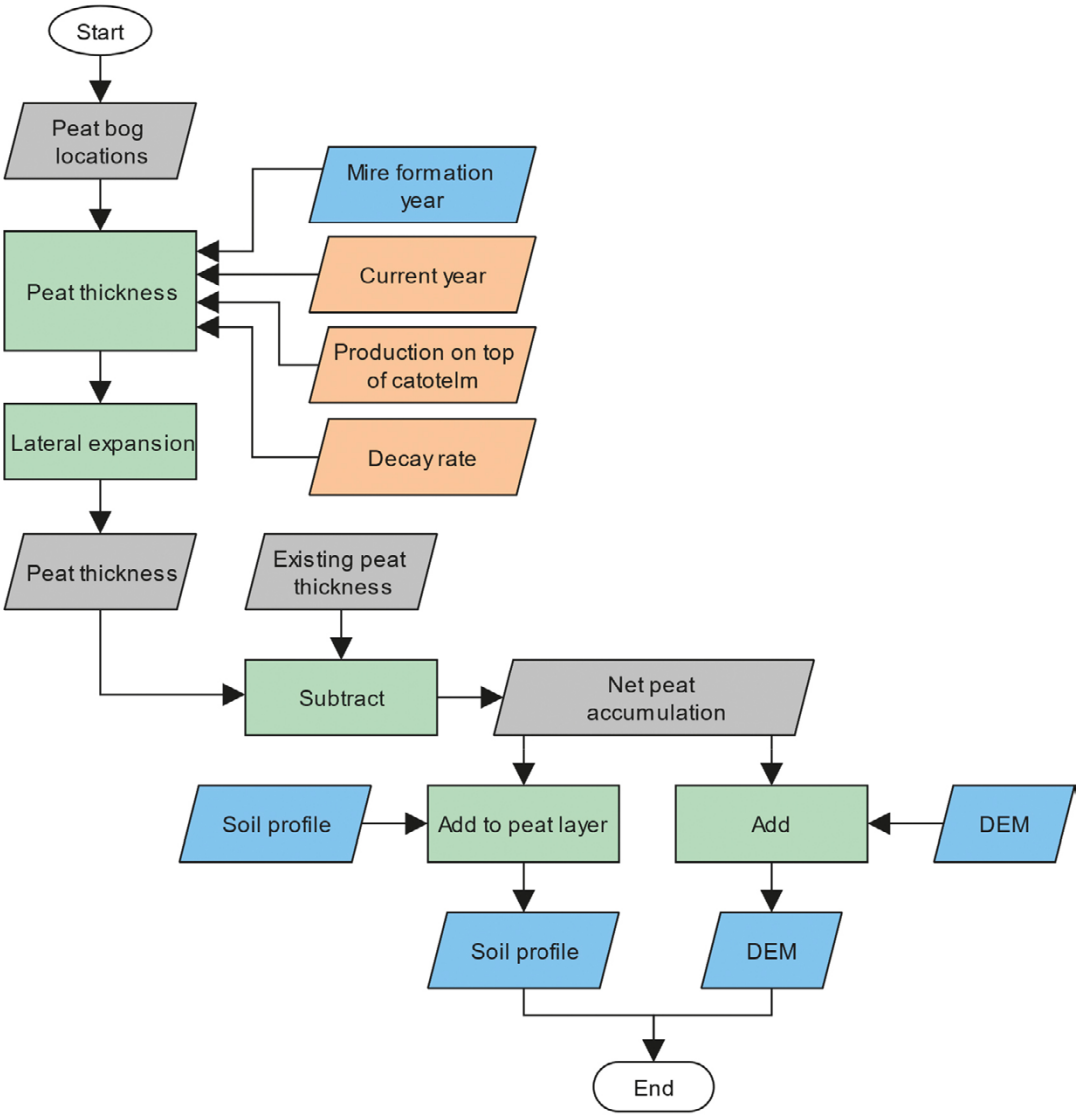

Figure 2-22. *Peat accumulation in raised bogs.*

2.3.2.1 Shoreline displacement

UNTAMO implements an empirical land uplift model developed by Påsse (2001). The model describes vertical displacement in terms of three distinct components: the *fast* and *slow* isostatic rebound and the eustatic sea level adjustment. The fast rebound is assumed take place immediately after the ice retreat and to dominate the overall rebound rate during a relatively short period thereafter. The slow rebound is much less pronounced and still ongoing. In the land uplift model, the slow component of the vertical shoreline displacement U_s (m) is approximated by an arc-tangent curve while the fast component U_f (m) is approximated using an exponential curve whose maximum value is defined by the time of de-glaciation T_f (calibrated year "*before present*" or *BP*)[1]:

$$U_s(t) = \frac{2}{\pi} A_s \left[\arctan\left(\frac{T_s}{B_S}\right) - \arctan\left(\frac{T_s - t}{B_s}\right) \right] \qquad (2\text{-}11)$$

$$U_f(t) = A_f \exp\left[-0.5 \left(\frac{t - T_f}{B_f} \right)^2 \right]$$

[1] In a later revision of the model (Påsse and Andersson, 2005), the exponential function has been replaced by an arc-tangent function for the fast component. UNTAMO uses the former definition although it would be trivial to implement the latter as the differences are insignificant.

where A_s and A_f (m) is half of the vertical displacement taking place for the slow and fast rebound components, B_s and B_f (1/y) are the inertia factors of the slow and fast rebound components and T_s, T_f (calibrated year BP) specify the time instant of the maximum rebound rate, typically associated with the time of the deglaciation taking place. The parameter t is likewise expressed in calibrated years BP.

The eustatic sea level change E (m) is given by

$$E(t) = \frac{2}{\pi} A_e \left[\arctan\left(\frac{T_e}{B_e}\right) - \arctan\left(\frac{T_e - t}{B_e}\right) \right] \tag{2-12}$$

$$E(t) = \frac{2}{\pi} A_e \left[\arctan\left(\frac{T_e}{B_e}\right) - \arctan\left(\frac{T_e - t}{B_e}\right) \right]$$

Vertical displacement at time t is then computed as

$$\Delta z(t) = U_s(t) + U_f(t) - E(t) - S(t). \tag{2-13}$$

Here $S(t)$ (m) is an optional term that accounts for sea level changes due to other factors such as climate-induced changes. An example land uplift curve is shown in Figure 2-23.

The amount of vertical displacement to be applied between two consecutive time steps $k-1$ and k is then calculated by evaluating Equation 2-13 at times t_{k-1} and t_k and taking the difference

$$\Delta z(t_{k-1}, t_k) = \Delta z(t_k) - \Delta z(t_{k-1}). \tag{2-14}$$

The computation of the shoreline displacement in the DEM, as implemented in UNTAMO, is shown in Figure 2-24.

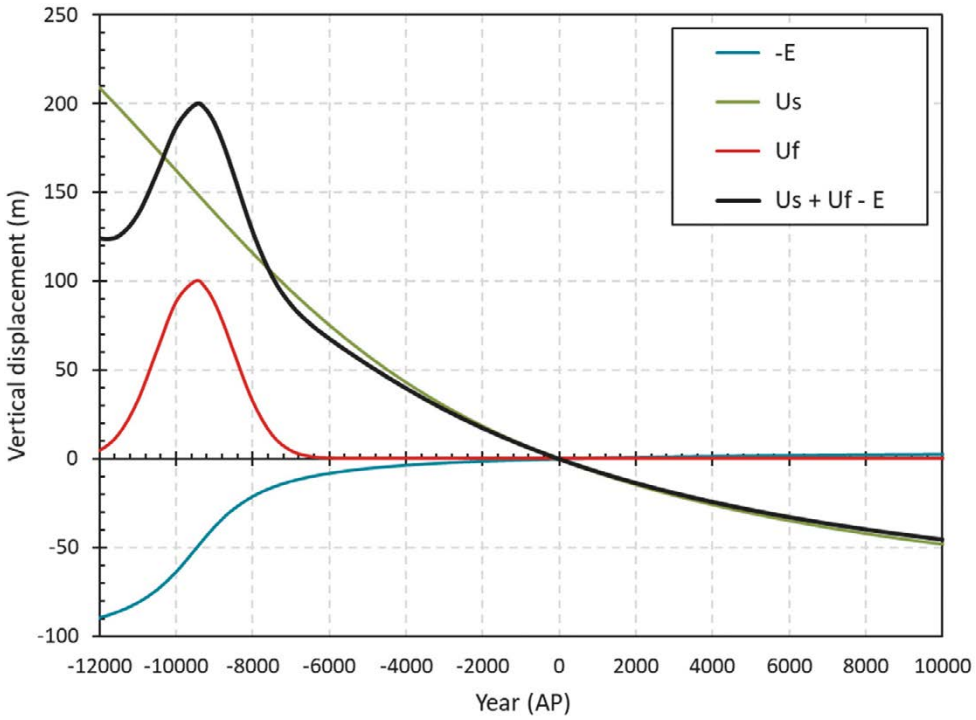

Figure 2-23. *Example of a land uplift curve for a theoretical location, including the Eustatic sea level rise (-E term), slow and fast land uplift components (Us, Uf) and the combined displacement (Us + Uf – E). Please note that the inverted form of the curve on the vertical axis is intentional – the land uplift model describes the amount of land uplift that shall happen from the given time until the present (0 AP). Therefore, the displacement due to land uplift is positive in the past (land is expected to rise since then till present) and negative in the future. The additional term S accounting for external sea level change is not shown. The values used are A_S = 270, B_S = 7 200, T_S = 10 000, A_f = 100, B_f = 1 000, T_f = 9 500.*

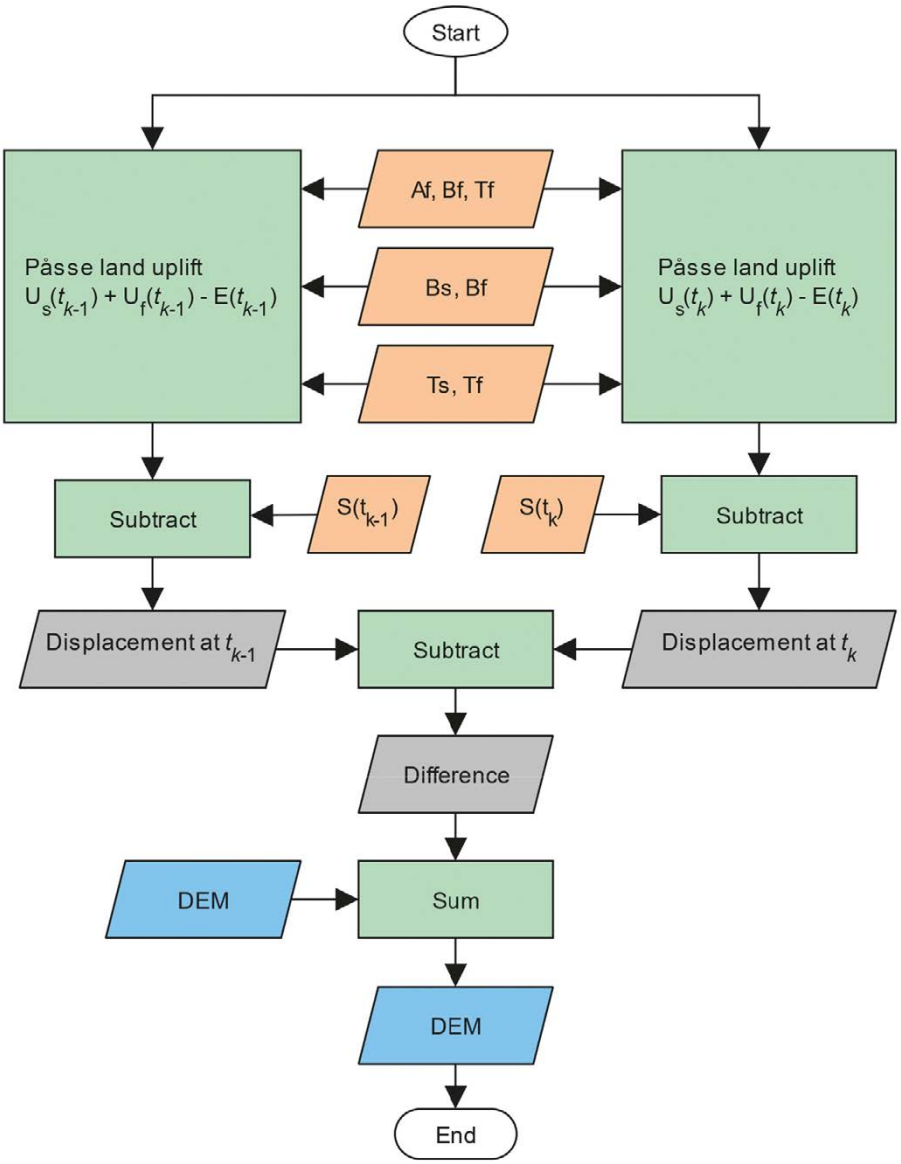

Figure 2-24. *Shoreline displacement applied to the DEM. The DEM is adjusted by the amount of land uplift occurring from the time t_{k-1} (previous time step) till t_k (current time step).*

2.3.3 Streamflow

UNTAMO uses the concept of accumulated flow to identify streams and rivers. The accumulated flow is computed from precipitation parameters and the DEM. Areas with sufficiently high accumulated flow will be classified as streams while areas where water collects (sinks) may become lakes or wetlands.

2.3.3.1 Computation of accumulated flow

The first step in the calculation of accumulated flow is to establish the surface runoff flow field using the DEM dataset. There are several methods for calculating the flow field from the DEM, with advantages and disadvantages to each. The D-8 method, originally put forward by Jenson and Domingue (1988), is used in UNTAMO. The D-8 method assumes that the surface runoff at each raster cell will proceed to the lowest-lying neighboring cell, including diagonally-placed neighboring cells. Therefore, water from each raster cell can flow in one of the eight possible directions, as shown in Figure 2-25, giving the method its name.

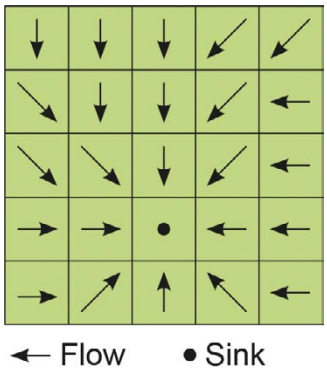

Figure 2-25. *Flow field computed using the D-8 flow direction algorithm.*

An advantage of the D-8 method is that it does not suffer from flow dispersion (a "splitting" of the preferential flow-paths when moving downstream) making it suitable for calculation of contributing area and for streamflow modelling. Other frequently used method for determining flow direction is the D-infinity method of Tarboton (1997) which does not restrict flow to eight compass directions. This method however can suffer from flow dispersion.

The D-8 and other gradient-based methods do not guarantee a continuous flow field over the model area. If none of the neighboring cells have lower elevation than the cell being examined then the cell is considered a hydrological sink. A common approach to help avoid this issue is to remove small, local depressions from the DEM by filling them up to a pre-determined threshold thus eliminating the sink. The algorithm used to "fill" the DEM in the UNTAMO model is explained in Planchon and Darboux (2002). This results in regions of zero gradient being created in the DEM and the gradient-based approach needs to be complemented by another technique to obtain continuous flow. Another approach is to compute the flow using the gradient approach until the sink is reached and then allow water to "flow upwards" or "cut through" the DEM to reach the outlet point of the depression. The latter approach is used by UNTAMO. UNTAMO uses the filled DEM to locate the nearest outlet of a depression and then a cost minimization technique to locate the path of least resistance to the outlet. The flow routing approach is illustrated in figures 2-26 and 2-27.

Before identifying streams and water bodies, the DEM is pre-processed so that soft sediment is removed. At the same time, hydrological sinks are filled to obtain a depression-less DEM as described earlier in this section. It is assumed that soft sediment is easily eroded by moving water and thus will not be found on river bottoms and in lake outlets. In UNTAMO, this is imitated by using a temporary DEM dataset with all soft sediment removed. The accumulated flow and lake boundaries (see Section 2.3.4.2) is then computed using this DEM instead. Sediments defined in the stratigraphy model (see Section 2.2.3) are classified as "soft" and "hard" by the user using the Lake.LowestSoftSediment parameter. The removal of soft sediment and creation of filled DEM is shown in Figure 2-28.

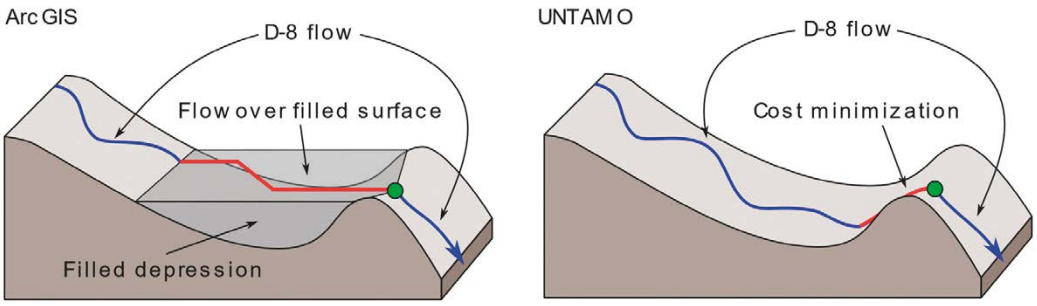

Figure 2-26. *Comparison of flow routing over a terrain with depression. Left) Flow direction approach used by ArcGIS. Right) Approach used by UNTAMO. Flow computed using the gradient (D-8 flow direction) is shown in blue, flow that cannot be computed from gradient is shown in red. The outlet of the depression is shown as a green dot.*

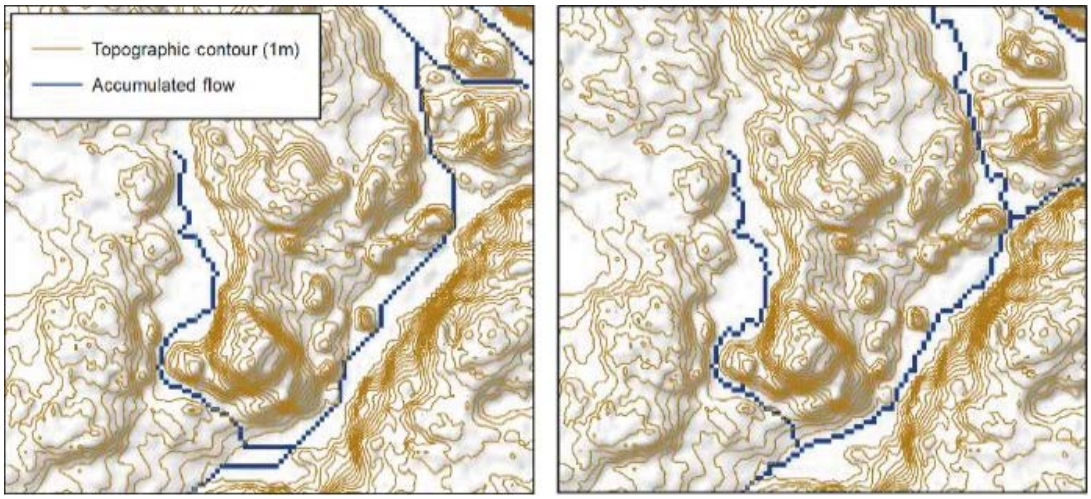

Figure 2-27. *Comparison of standard flow routing and UNTAMO flow routing over low slope areas. Left: Accumulated flow using Flow Direction and Flow Accumulation tools from ArcGIS. Right: Accumulated flow calculated by UNTAMO.*

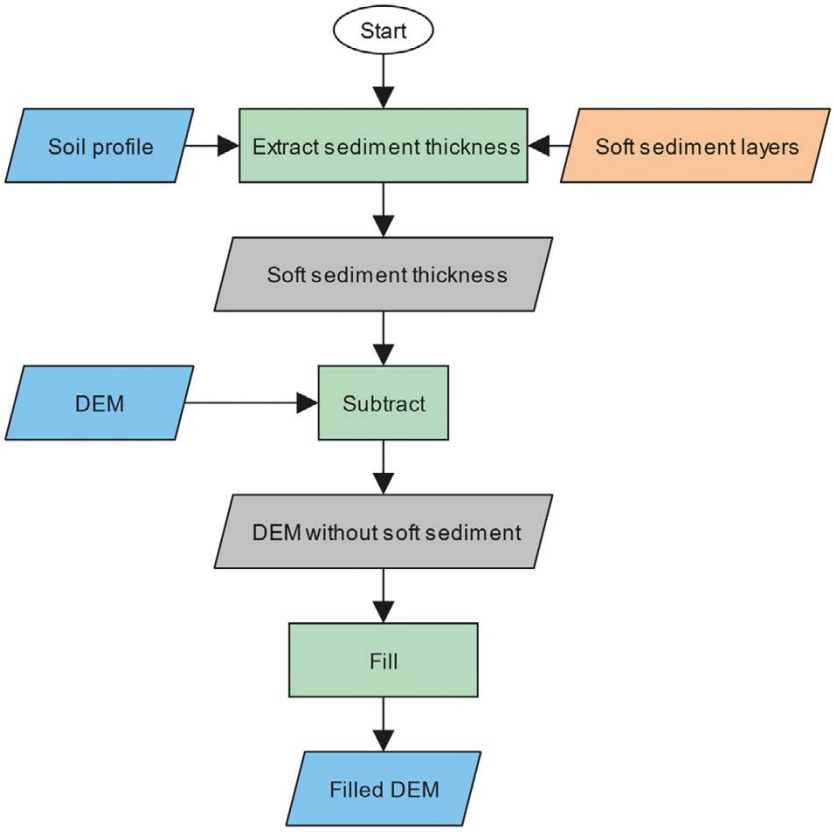

Figure 2-28. *Soft sediment removal and computation of filled DEM.*

UNTAMO does not use a coupled hydrological model in order to estimate the hydrological response to precipitation. Instead, UNTAMO estimates the mean discharge (Q, m^3/s), mean high discharge (Q_{MH}, m^3/s) and mean low discharge (Q_{MN}, m^3/s) of a watercourse given an assumed annual precipitation. The mean discharge Q is computed using the flow accumulation approach described above. The contribution of each cell, denoted Q_{cell}, to the accumulated flow is simplified using the rational method of Mulvany (1851) and is computed as

$$Q_{cell} = P\ P_{eff}\ A_{cell}\ 3.1536 \times 10^{-10} \quad (2\text{-}15)$$

where P (mm/a) is the annual precipitation sum, P_{eff} (-) is the runoff coefficient (also called the effective precipitation fraction), A (m^2) is the cell area and the constant is used for conversion to m^3/s. The runoff coefficient describes the fraction of precipitation that is not intercepted by vegetation or evaporated and is thus contributing to the streamflow and is determined empirically. The mean high discharge is defined as the mean of the yearly discharge maxima and is assumed to correspond to the bank-full discharge. Similarly, the mean low discharge is defined the mean of yearly discharge minima. Both are approximated from Q as

$$Q_{MH} = S_{MH} Q \quad (2\text{-}16)$$
$$Q_{MN} = S_{MN} Q$$

where S_{MH} and S_{MN} (dimensionless) are the mean high and mean low discharge scaling factors given by the user as input.

$$V = \frac{1}{n} R_h^{2/3} \sqrt{I}, \quad (2\text{-}17)$$

Boundary condition for discharge can be given to inject additional discharge into the modelled area during the flow accumulation calculation. This may be necessary if the UNTAMO model grid does not contain complete watersheds. A discharge boundary condition is specified the coordinates where the water will be injected and associated discharge data,. The computation of accumulated flow in UNTAMO is shown in Figure 2-29.

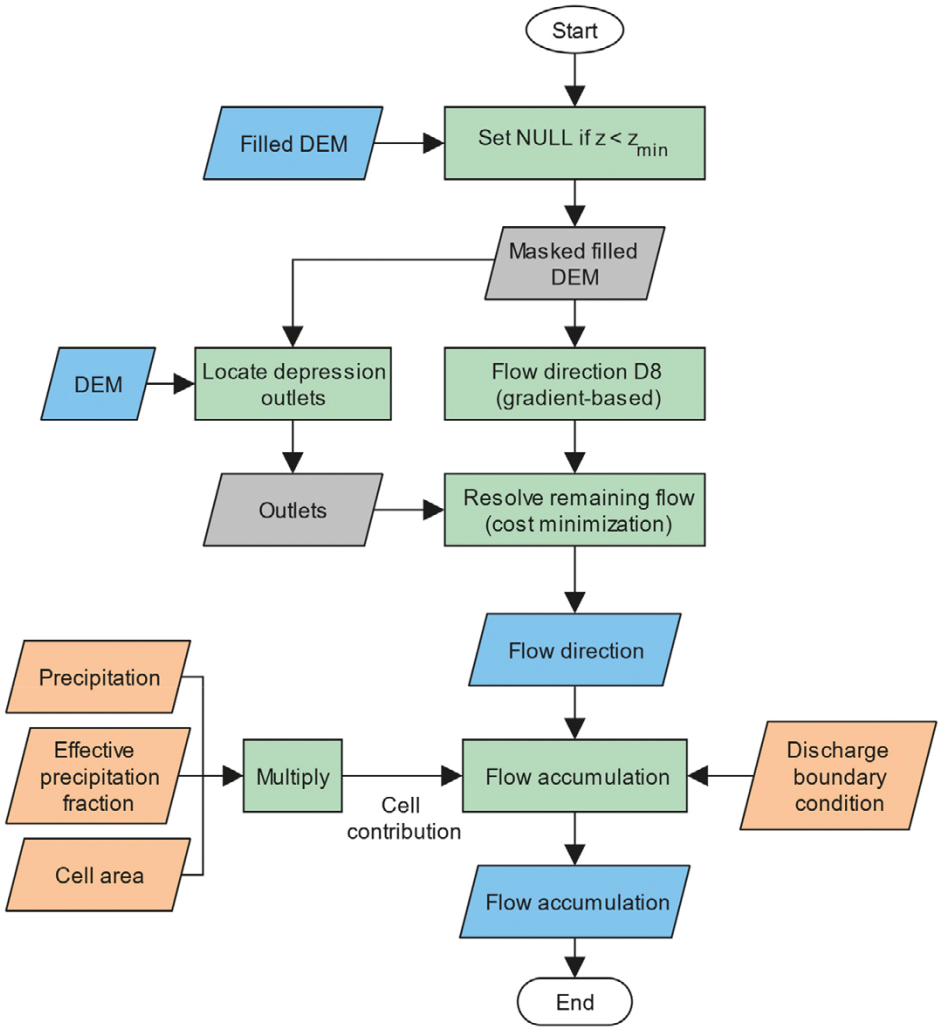

Figure 2-29. *Computation of accumulated flow from DEM and precipitation data.*

2.3.3.2 Stream network

Streams are identified from the flow direction and accumulation data as shown in Figure 2-30. Pixels with accumulated flow higher than a given minimum discharge (parameter Streamflow.DischargeThreshold) are extracted and the resulting binary mask is traced, and converted to a network of stream segments as shown in Figure 2-31. A stream segment ends when its length has exceeded the a user-defined length (the Streamflow.MaxSegmentLength parameter) or when junction point in the network is reached. Finally, attributes for each segment are calculated, including the accumulated discharge (m^3/s), elevation (m above sea level) and gradient (degree). Additional attributes describing the stream channel geometry are also calculated as described in Section 2.3.3.3.

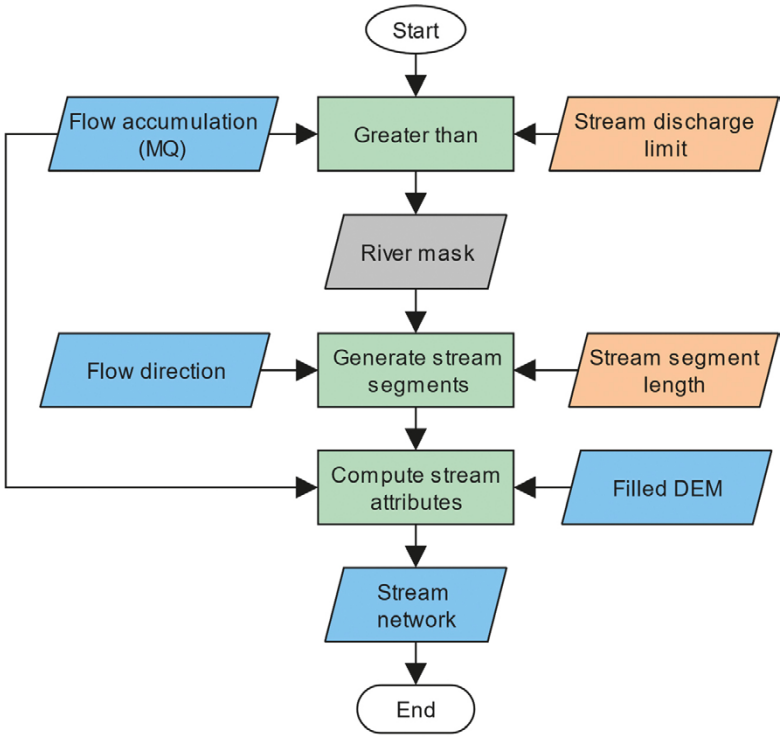

Figure 2-30. *Derivation of stream network from flow direction and accumulation data.*

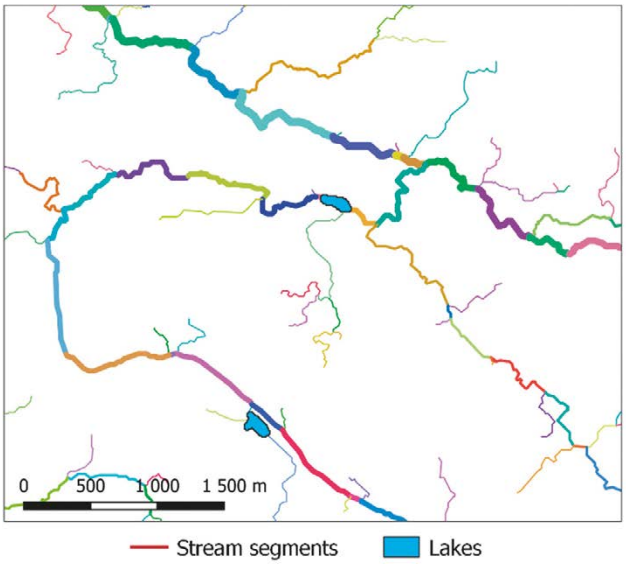

SEG_Length	840,83261120700
Elevation	10,55319290160
Slope	0,00144048234
Q_MQ	0,12242040783
Q_MNQ	0,0181181971
Q_MHQ	0,41035321355
BSlope	-1,00000000000
CSType	ELLIPTICAL
Width_MHQ	3,34466534269
Depth_MHQ	0,2099609375
CSArea_MHQ	0,55154513059
WPerim_MHQ	3,42109214308
Width_MNQ	2,13593391460
Depth_MNQ	0,04838943481
CSArea_MNQ	0,07066725883
WPerim_MNQ	2,13895938528
Width_MQ	3,00758465351
Depth_MQ	0,11810302734
CSArea_MQ	0,25441489365
WPerim_MQ	3,02198790572

Figure 2-31. *Example of the streamflow segment network derived from flow accumulation data. Individual segments are shown in different colours, the desired segment length has been set to 1km. The line width of the segments on the map correlates with the mean discharge. An example of the segment attributes that are stored for each segment is provided on the right-hand side.*

2.3.3.3 Stream channel geometry

The cross-section dimensions of rivers and streams are calculated using the Manning equation for open flow (Manning et al. 1890) according to equation

where V (m/s) is the cross-sectional average velocity, n (dimensionless) is the Gauckler-Manning coefficient, R_h (m) is the hydraulic radius and I (m/m) is the hydraulic head loss or energy slope. The channel is assumed to be determined by events that occur at or near the bank-full discharge and its dimensions are therefore computed by substituting the discharge formula $Q_{MH} = AV$ for the cross-sectional velocity. Equation 2-17 can then be rewritten as

$$Q_{MH} = \frac{1}{n} A R_h^{2/3} \sqrt{I}, \tag{2-18}$$

where A (m^2) is the cross-section area. The hydraulic radius is a measure of the channel flow efficiency and can be further expressed as

$$R_h = \frac{A}{P}, \tag{2-19}$$

where P (m) is the wetted perimeter (the perimeter of the cross-section that is in contact with water). The energy slope I depends on the discharge, the longitudinal slope of the channel bottom, shape of the cross-section and other factors. In UNTAMO, the energy slope is assumed equal to the topographic elevation drop Δz over a predefined distance Δl as

$$I = \frac{\Delta z}{\Delta l}. \tag{2-20}$$

As an example, energy slope $I = 0.01$ in UNTAMO corresponds to a 1 metre drop in channel elevation per 100 metres of the channel length. To avoid problems with zero slope on flat areas, a minimum value for I can be enforced.

The cross-section area A_{MH} needed to convey the known discharge Q_{MH} is calculated by setting A to A_{MH} in Equation 2-18 and then solving for A_{MH}. UNTAMO assumes either a trapezoidal or elliptical channel geometry; the distinction is made based on the soil type at the channel bottom and the mapping between soil types and the assumed channel geometry is given by the user. The trapezoidal and elliptical channel geometry is shown in Figure 2-32.

The depth of the channel d_F (m) corresponding to the full-bank stage is then calculated as

$$d_F = \begin{cases} \frac{s}{2}\left(w_F + \sqrt{w_F^2 - \frac{4A_{MH}}{s}} \right) & \text{for trapezoidal channels} \\ \frac{2A_{MH}}{\pi w_F} & \text{for elliptical channels,} \end{cases} \tag{2-21}$$

where w_F (m) is channel width at the bank-full stage and s (m/m) is the slope of the immersed bank given as the vertical drop per unit horizontal length (i.e. $s = \Delta z/\Delta x$). Given the channel geometry type (trapezoidal or elliptical), the wetted perimeter P in Equation 2-19 is defined using Equation 2-22 for the trapezoidal cross-sections and Equation 2-23 for the elliptical cross-section:

$$P = \left(\sqrt{s^2 + 1} - 1\right)\frac{2D}{s} + W \tag{2-22}$$

$$P = \frac{\pi}{2}\left[3\left(\frac{W}{2} + D\right) - \sqrt{\left(\frac{3W}{2} + D\right)\left(\frac{W}{2} + 3D\right)}\right] \tag{2-23}$$

The wetted perimeter for elliptical channels, given in Equation 2-23, is based on Ramanujan's approximation for the circumference of an ellipse (Ramanujan et al. 1962).

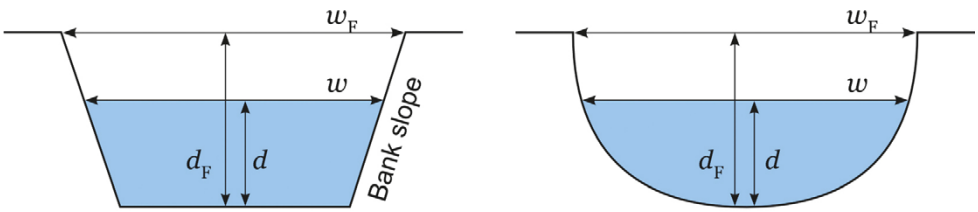

Figure 2-32. *Left) trapezoidal channel, right) elliptical channel.*

The full-bank channel width is estimated from the mean-high discharge using a power relation suggested by Leopold and Maddock (1953) of the form

$$w_F = \alpha Q_{MH}^{\beta} \tag{2-24}$$

The model coefficients α and β are determined empirically.

The water depth d (m) and cross-section width w (m) for other discharge conditions $Q < Q_{MH}$ are then computed from the channel geometry so that the cross-section area A necessary to convey the discharge Q, given by Equation 2-18, is satisfied.

2.3.4 Waterbody identification

2.3.4.1 Identification of sea

In UNTAMO, the DEM always contains elevation relative to the sea level. The sea can therefore be easily identified as all areas where elevation is less than 0. In general, terrestrial areas may exist below the sea level or a low-lying basin may contain a freshwater lake. For this reason, UNTAMO requires sea to always be marked with a set of spatial coordinates so that only regions that are at or below the sea level and intersect with at least one sea marker are classified as sea. Sea markers are placed before running the model (they are not time-dependent) at locations within the model that are expected to contain the sea. Additional markers may need to be placed afterwards if parts of the sea are incorrectly classified as being terrestrial or lake. This typically happens at the model grid boundary because no information is provided to UNTAMO regarding areas beyond the model boundary. The use of sea marker points is illustrated in Figure 2-33.

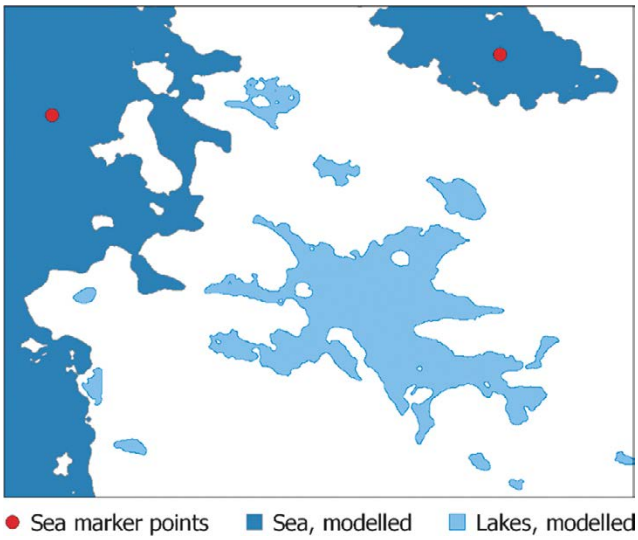

Figure 2-33. *Usage of sea marker points to correctly classify marine and freshwater environments within the modelled area. In this example, the boundary of the figure represents the boundary of the modelled area. The large body of water near the centre of the figure is classified as a lake even if its surface is below the sea level because it does not contain any sea marker. The large water bodies which are cut off by the model area boundary are correctly classified as sea because each of them intersects with a sea marker point.*

The sea boundary can be generalized to remove unwanted complexity due to noise in the DEM. The generalizing filter can also be used to prevent parts of rivers being incorrectly classified as sea if the channel bottom elevation is below zero, as shown in Figure 2-34. Shoreline generalization is done using a morphological opening filter applied to the binary sea mask. With a large enough filter radius, narrow parts of the sea mask are removed and may be classified as rivers or lakes instead. The filter can be adjusted using the Sea.MinimumFragmentWidth parameter and can be disabled completely by setting this parameter to zero. The complete sea delineation algorithm is illustrated in Figure 2-35.

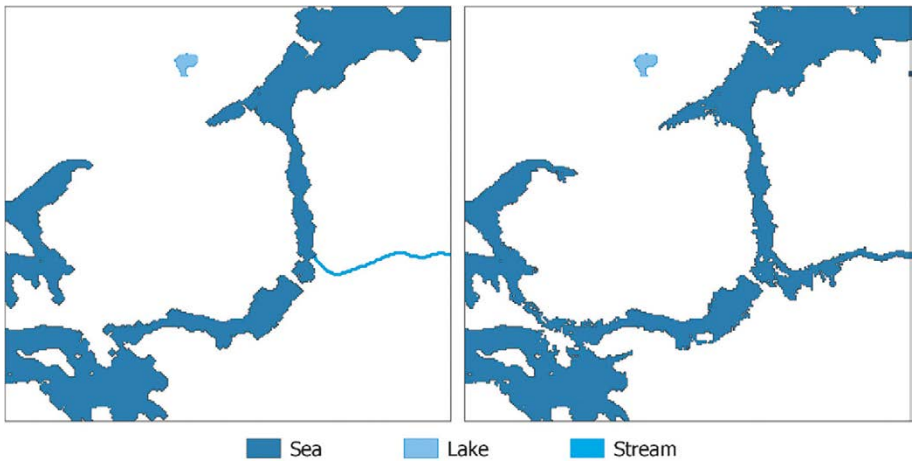

Figure 2-34. *Example of the effect of shoreline generalization. Left: Sea shoreline after generalization using 20-metre width limit. The generalization leads to a loss of small detail but river flowing into the sea from the east is correctly classified. Right: Sea shoreline without generalization, the river is incorrectly classified as sea.*

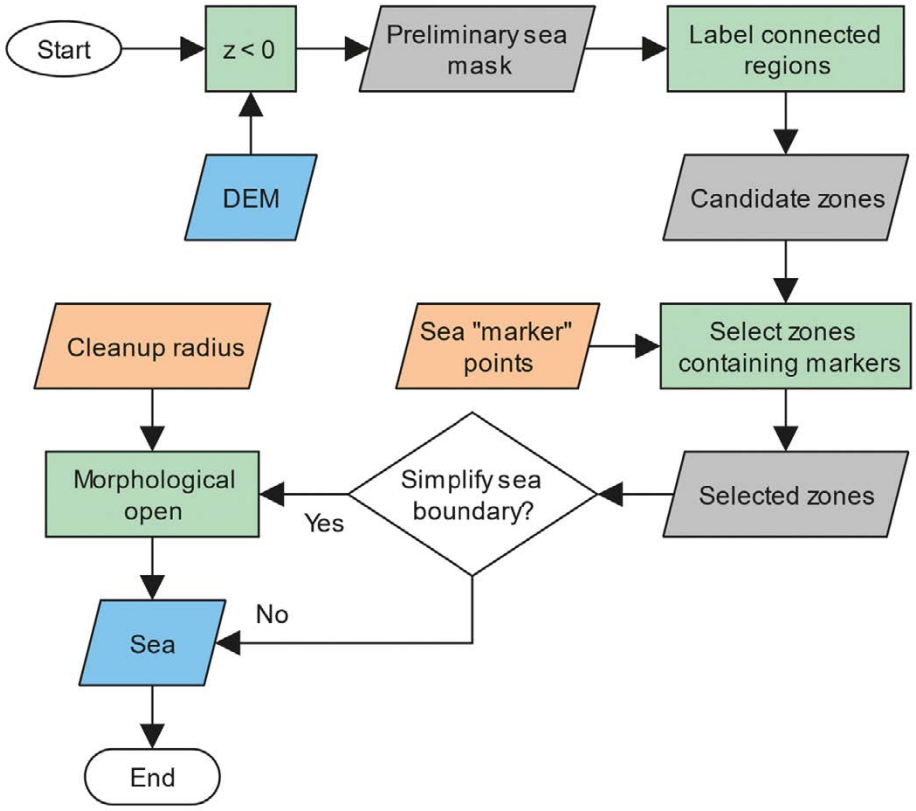

Figure 2-35. *Identification of sea from the DEM.*

2.3.4.2 Identification of lakes

To delineate lakes, the depth of standing water is calculated first by taking the difference between the original and filled DEM. Due to the limited spatial resolution of the DEM, the elevation at the lake outlet derived from the DEM might be slightly higher if the cross-section of the outlet is narrower than the DEM cell size. This is due to the fact that the elevation of the surrounding areas is likely at higher elevation and the spatial averaging resulting from large cell size is thus biased towards higher elevation. The higher outlet elevation may in turn lead to UNTAMO giving higher estimate of water depth and the overall water volume than it otherwise would have given if supplied with a DEM with a higher spatial resolution. UNTAMO can compensate for this by removing sediment from the lake outlet using the river incision module described in Section 2.3.5. The theoretical channel depth, derived from discharge, is then removed from the DEM before lakes are identified. Furthermore, easily erodible sediments such as peat or gyttja can also be automatically removed from the outlet, as described in Section 2.3.3.

The determination of lake threshold elevation is illustrated in Figure 2-36. The computation of water depth is shown in Figure 2-37.

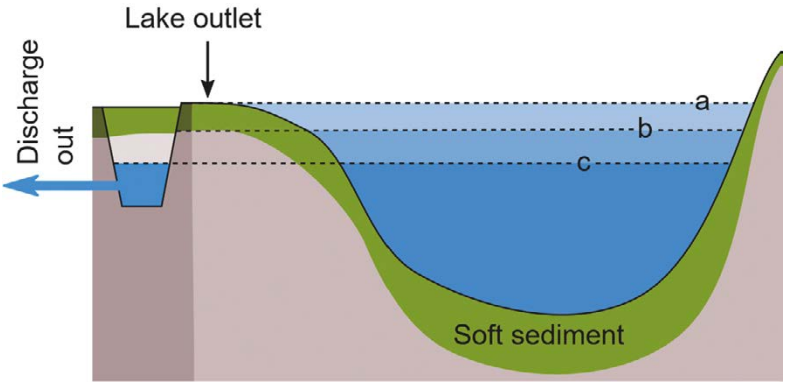

Figure 2-36. *Determination of lake water surface elevation: a) threshold elevation determined from original DEM, b) threshold elevation after removal of soft sediment from DEM, c) final water surface elevation after removal of soft sediment and the river channel and counting for the flowing water depth in the outlet.*

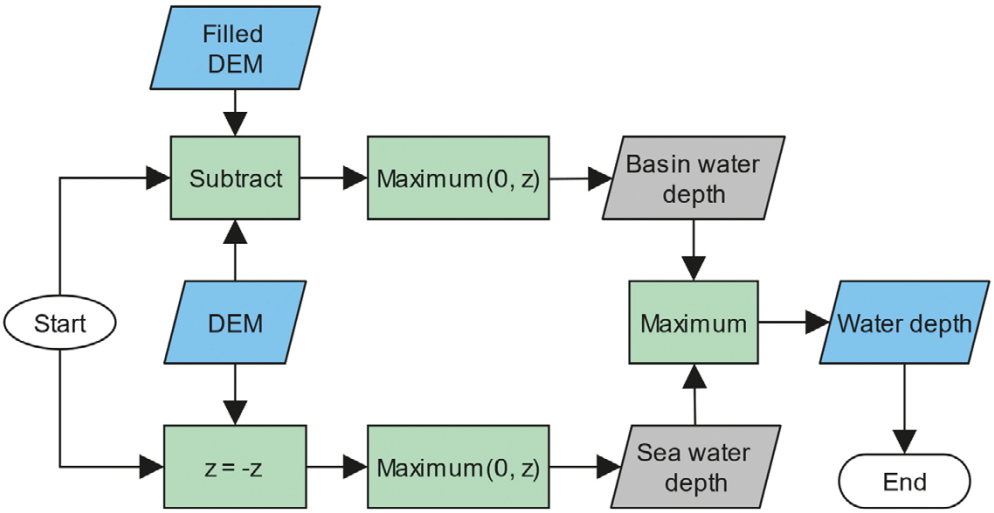

Figure 2-37. *Computation of standing water depth from DEM. The final dataset contains both the sea and lake water depth, terrestrial areas have a value of zero.*

Because the location and extent of lakes must be known for river incision and lake threshold erosion to be applied, UNTAMO first identifies an initial, temporary set of lakes. The preliminary lakes are used by the threshold erosion and incision module and final lakes are identified afterwards as shown in Figure 2-38.

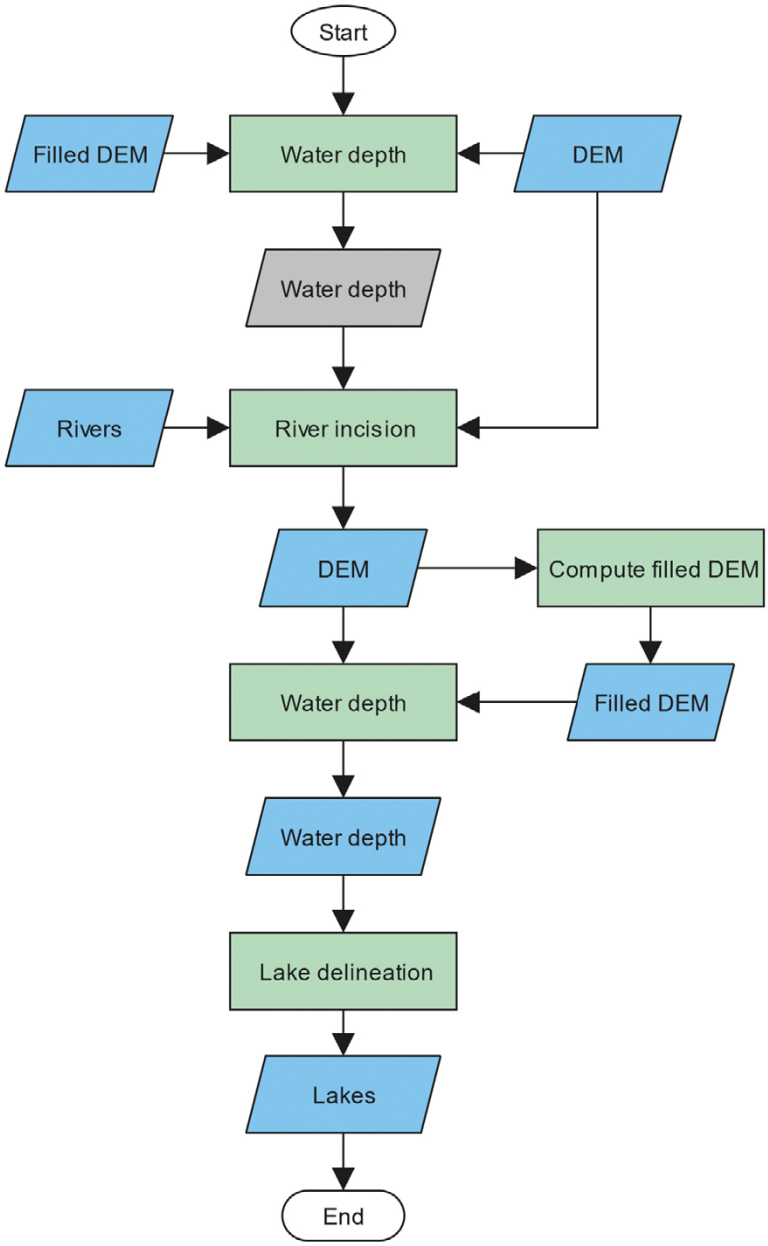

Figure 2-38. *River incision and erosion of lake threshold before lakes are delineated.*

Lake delineation proceeds by identifying areas with water depth greater than given minimum depth (Lake.MinimumWaterColumnDepth parameter), resulting in a lake mask containing potential lake locations. Similarly to the sea shoreline, the lake mask boundary can be simplified using a generalization filter to remove unwanted detail and very narrow features that should rather be classified as rivers. The function and parametrization of the filter is identical to the sea shoreline filter described in Section 2.3.4.1. The final binary lake mask is converted into a set of discrete objects so that pixels that are spatially connected constitute a single object (lake). The objects represent "candidate" lakes from which the final set of lakes is selected by the following criteria:

- Average depth – average depth of the lake must be greater or equal to a given limit (parameter Lake.MinimumMeanDepth)
- Surface area – surface area of the lake must be greater or equal to a given limit (parameter Lake.MinimumSurfaceArea)
- Surface elevation – surface elevation (water level) of the lake must be greater or equal to a given limit (parameter Lake.MinimumSurfaceElevation)
- Minimum volume – water volume of the lake must be greater or equal to a given limit (parameter Lake.MinimumWaterVolume)
- Minimum diameter – "diameter" of the lake must be greater or equal to a given limit (parameter Lake.MinimumDiameter)

The criteria listed above are optional and only those that are specified are evaluated. A candidate lake is selected if all specified criteria are met. The diameter of a lake is computed as the diameter of the largest circle that can be fitted inside the lake boundary. The diameter criteria can be used to prevent formation of long but very narrow lakes (such that their surface area or water volume satisfies the selection criteria) if such features should rather be classified as rivers. While somewhat arbitrary, the minimum diameter criteria may be needed if parts of rivers are erroneously classified as lakes. In the future, the lake identification could be improved to classify lake and river ecosystems correctly without the need for such workarounds. The lake delineation algorithm is shown in Figure 2-39.

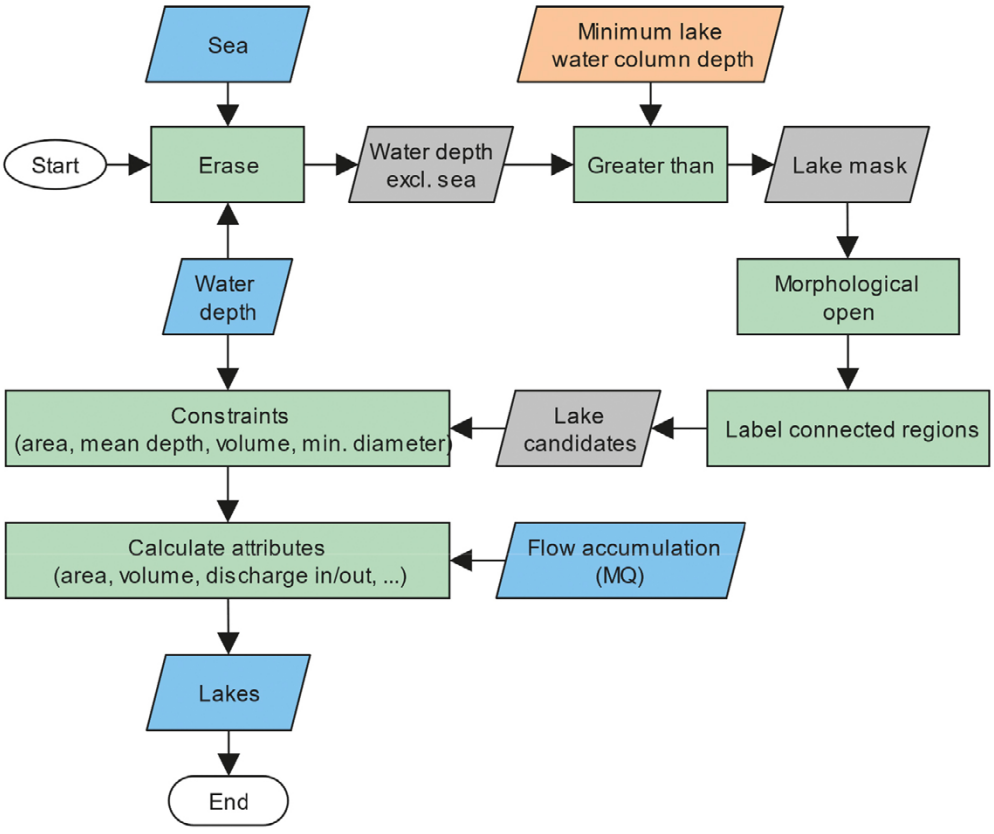

Figure 2-39. *Identification of lakes from DEM.*

2.3.4.3 Classification of lake edge mires

In UNTAMO, lake edge mires represent a type of wetlands found near lake shores where ground-water table is near the surface, or the area is submerged (either permanently or periodically) but water is sufficiently shallow to allow for peat forming vegetation to grow. In UNTAMO, lake margins where water depth is below the lake classification criteria (see Section 2.3.4.2) are always classified as mires and filled immediately with peat up to the threshold level of the lake. Please note that this does not mean that all depressions are filled with peat up to the threshold level. Only terrain depressions where lake exists will contain mires near the lake edges. Elsewhere, mires may develop, if suitable conditions prevail, in the form of raised peat bogs as described in Section 2.3.2.

The approach for classification of lake edge mires is shown in Figure 2-40. The algorithm first locates areas of shallow water that touch or intersect with a lake. Lakes within both the current and previous time step are considered. This is to account for potentially significant changes to the lake between timesteps.

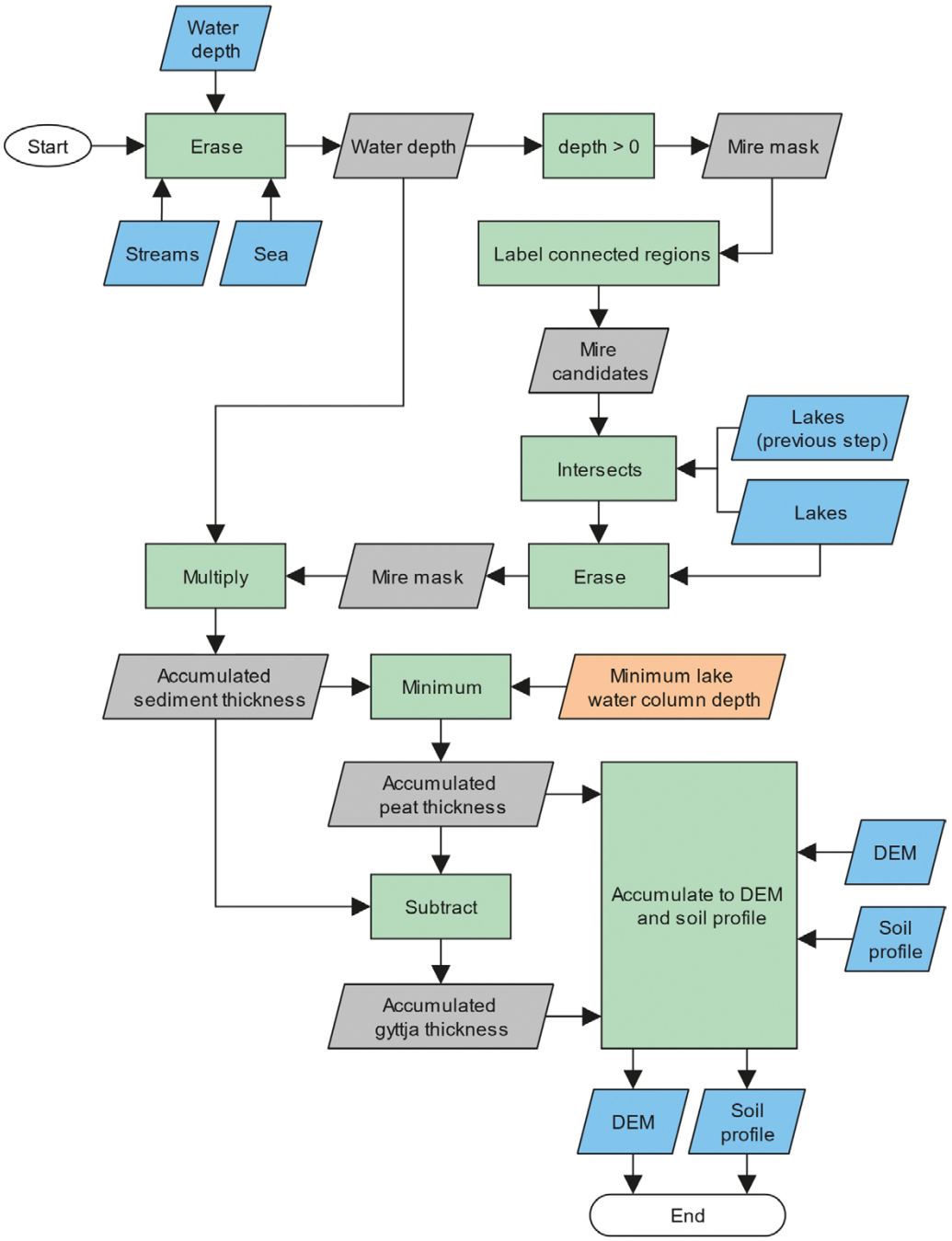

Figure 2-40. *Classification of lake edge mires after lakes have been delineated. The mires are filled instantly with organic sediment (gyttja and peat) up to the lake water level.*

Lake terrestrialization, and subsequent mire formation, are processes that are continuously ongoing. The relatively coarse temporal discretization used by UNTAMO may however cause a lake shoreline to move dozens of meters between two consecutive time steps, or the lake may become fully overgrown from one time step to the next. For this reason UNTAMO considers also lakes from the previous iteration and for any pixels that are transitioning from a lake (previous time step) to a lakeside mire, the remaining depth up to the threshold level is filled with organic sediment first (in accordance with the vegetation in-filling module described in Section 2.3.1.2), the remaining top layer is filled with peat as shown in Figure 2-8 in Section 2.1.1.

2.3.4.4 Classification of littoral zones

"Littoral zone" is considered the part of a sea or lake colonized by dense aquatic vegetation, the remaining part of the sea or lake is considered open water. The littoral zone is defined both by the maximum water depth that allows roots of aquatic plants to take hold (parameters Reed.MaxDepthForGrowthLake and Reed.MaxDepthForGrowthSea, typically up to 2 meters) and by physical exposure to disturbance caused by wave action. If the stress exerted on the lake or sea bottom due to water movement becomes strong enough, organic sediment will eventually be eroded away and the area will become unsuitable for the vegetation to grow. In UNTAMO, the disturbance due to wave action at the bottom is simplified by modelling the average fetch distance across open water in 360-degree circle. This is done by projecting multiple lines from each cell (UNTAMO uses one-degree interval, resulting in 360 lines per cell) and evaluating the distance to its nearest intersection with shoreline. The average fetch distance can be optionally be weighted by the probability of wind blowing from each direction (parameter Reed. WindProbability, given separately for each of the eight compass directions).

Each cell inside the sea or lake is classified as littoral zone if the water depth is below the given limit and mean fetch distance is below the fetch distance limit (parameters Reed.ReedFetchThresholdLake and Reed.ReedFetchThresholdSea). The usage of fetch distance as a proxy for shoreline exposure is illustrated in Figure 2-41. The complete littoral zone classification algorithm is presented in Figure 2-42.

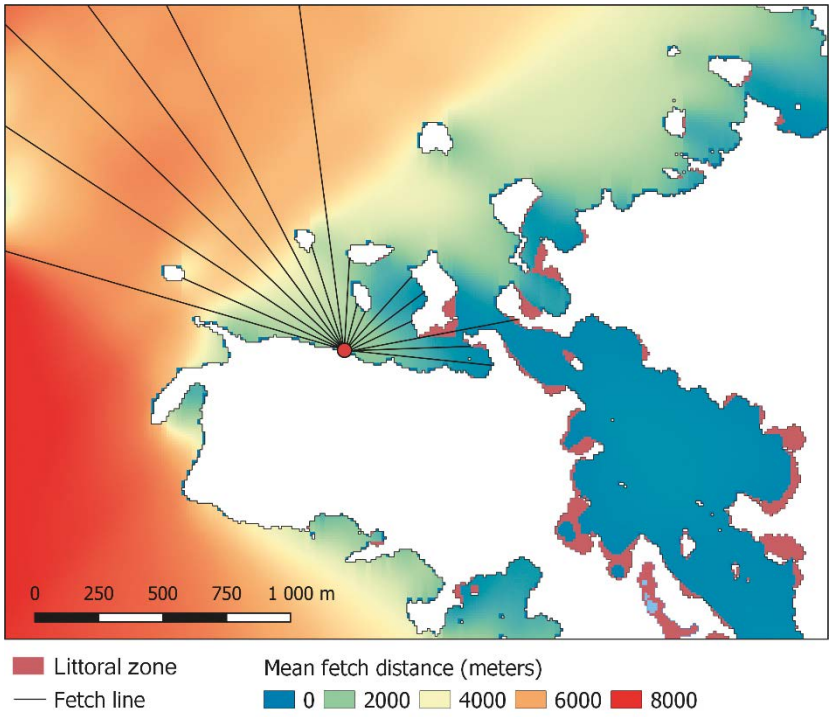

Figure 2-41. *Mean fetch distance as a proxy indicator of shoreline exposure. Growth of aquatic vegetation is limited to shallow areas with sufficiently short mean fetch distance. The fetch lines shown on the map illustrate how the mean fetch distance is calculated for a single location (marked with the red circle), the background color shows the computed mean fetch for the entire area.*

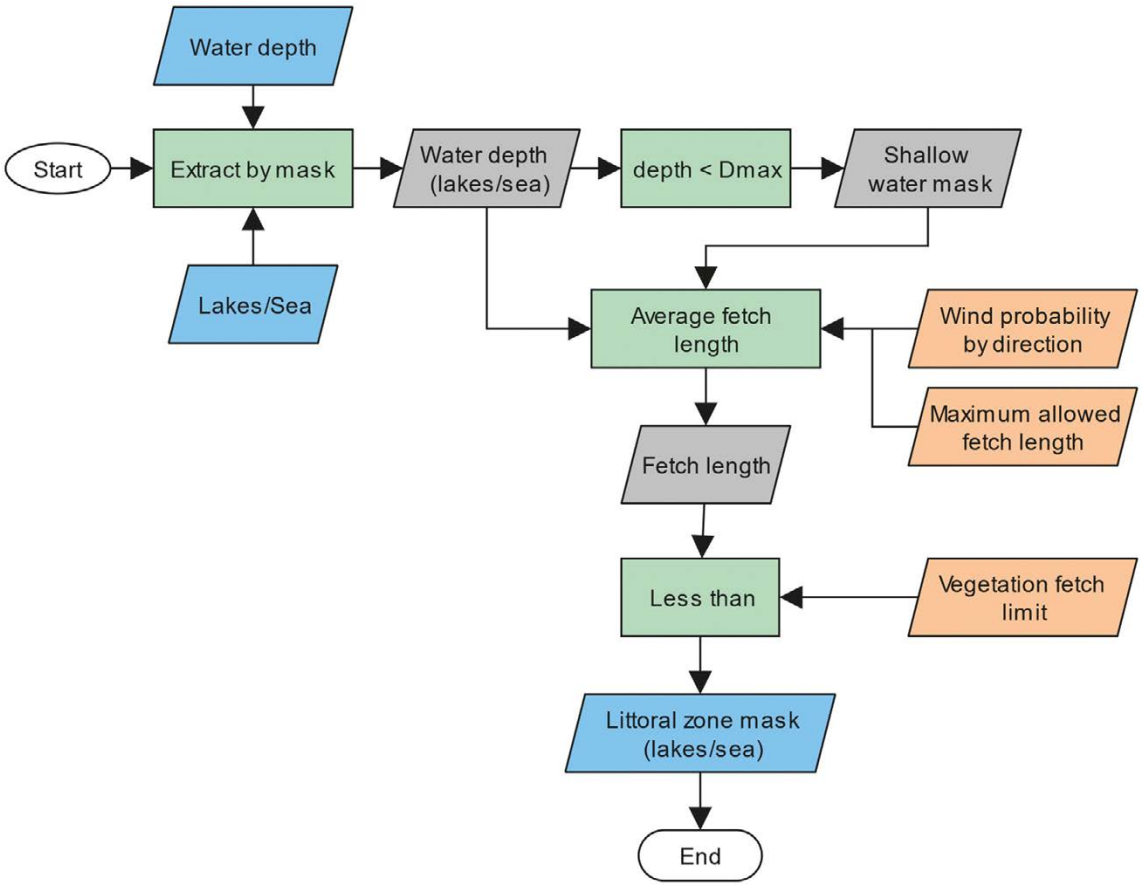

Figure 2-42. *Classification of littoral zones for lakes or sea. The algorithm is identical for both cases, but parameter values can differ.*

2.3.5 River incision

River incision refers to the narrow erosion of river channel due to the sheer force of the moving water. River incision was originally implemented in UNTAMO to prevent river channels from unexpectedly changing course because of small differences in DEM cell values caused by gradual tilting of the landscape (occurring when parameters for the shoreline displacement module have a spatial trend). Second purpose of the incision module is to allow further erosion of lake outlets beyond removal of soft sediments (described in Section 2.3.4.2). The incision module is however not designed to produce a "natural looking" landscape as only one cell -wide channel is eroded along the stream network.

The incision of the river channel is assumed to be a relatively fast process, in comparison to the model time step, and is therefore applied instantly rather than being modelled as a continuous and time-dependent process. The incision is only applied on newly formed land (following the exposure of land due to shoreline displacement or when a lake is overgrown) or when a river or stream changes course. The river channel is eroded up to the depth given by the channel geometry equations in Section 2.3.3.2. All sediment types can be eroded except for the bedrock, which is never eroded by moving water. UNTAMO tracks, at every model grid cell, the total amount of sediment eroded by the river incision module. This is used to prevent the incision being applied repeatedly to the same area (due to the fact that it is not being modelled as a time-dependent process). The effect of river channel incision on the DEM is shown in Figure 2-43, the algorithm is shown in Figure 2-44.

Figure 2-43. *Hillshade of a terrain with eroded river channel. The channel centreline is shown as blue dashed line.*

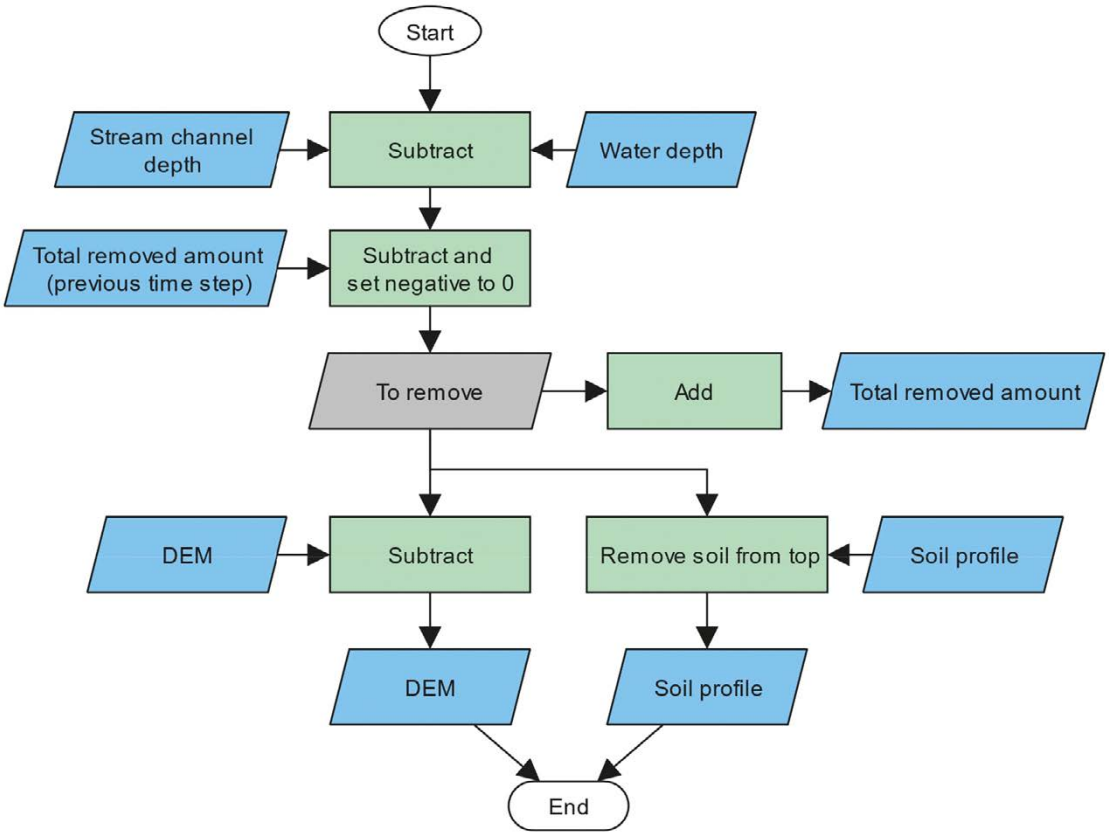

Figure 2-44. *Incision of stream channels into the DEM and soil profile data.*

2.3.6 Land use

The land use module of UNTAMO contains two sub-modules: the agricultural land allocation module and the mire drainage module. Both modules handle human induced changes to the landscape and are not modelled using a physical model. Instead, the models of the land use changes are stylized in nature and current agricultural and land management practices are used as a basis for the models. Both modules can be configured to simulate various scenarios such as present-day practice, intensive agriculture (all suitable land converted to cropland) or nature conservation (minimal agriculture, no peatland drainage). Changes to the landscape are assumed to occur at a much smaller time-step than that used by the rest of the model and are therefore applied instantly during the landscape feature identification stage (see Figure 2-4).

Both modules use parameters (such as the desired cropland or natural peatland area) defined as a fraction of the terrestrial area. The algorithm for computation of the terrestrial land area is outlined in Figure 2-45.

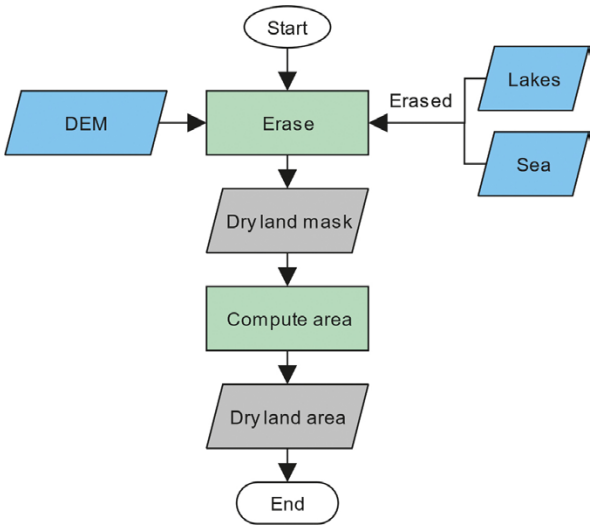

Figure 2-45. *Computation of dry land mask and area used in the agricultural and drainage sub-modules.*

2.3.6.1 Agricultural land allocation module

The purpose of the agriculture module is to allocate land for agricultural use, including for example cultivation of crops and animal grazing. The outcome of the allocation procedure is a set of "field plots", which are small patches of land that roughly resemble those in use today as shown in Figure 2-46. It is possible to define multiple crop types that shall be cultivated (other use such as grazeland can be thought of as a "crop type" in UNTAMO) and give parameters for each crop type separately. UNTAMO will then allocate field plots for each crop type, based on their parameters. If the aim is only to classify agricultural land without distinguishing different crop types, a single generic crop type can be defined and used instead.

The identification of agricultural land and delineation of field plots is based on a *suitability index* of each grid cell for cultivation. The suitability index ranges from zero (unsuitable) to one (most suitable) and is based primarily on the suitability assigned to the soil in the top layer (Agri.SoilSuitability parameter). The soil -related suitability is also specific to crop type (separate values are given for each soil type and crop type combination) and the resulting suitability index is therefore also crop type -specific. Non-terrestrial areas are excluded from the suitable land (suitability index is set to zero). Land which can be infiltrated with saline water from the sea can also be excluded by specifying minimum elevation above the sea level required for croplands (parameter Agri.MinElevation). The computation of the suitability index is shown in Figure 2-47.

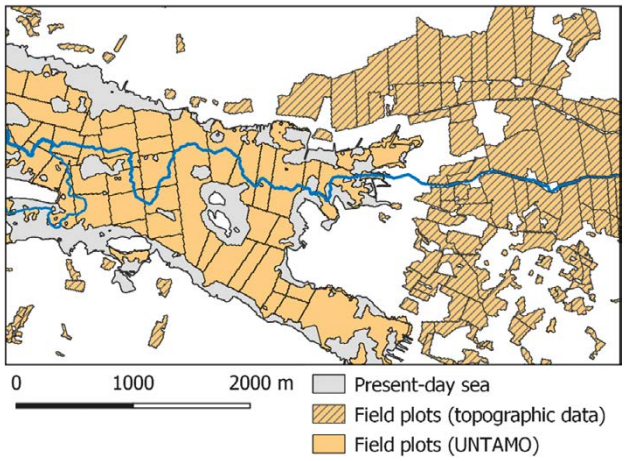

Figure 2-46. *Field plots generated by UNTAMO (plain yellow) compared to existing field plots digitized from topographic data (yellow, hatched). The land that emerged from the sea that has subsequently been cultivated is shown in grey. Topographic data from Land Survey of Finland (NLS 2022).*

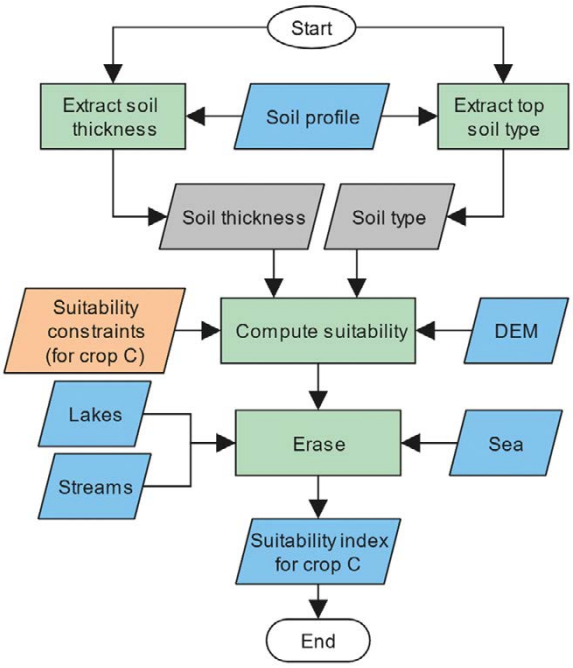

Figure 2-47. *Computation of suitability index for agriculture for a single crop type (denoted C in the flowchart).*

The suitability index is then used to identify all land that can be suitable. This includes all areas where the suitability index is greater than zero, resulting in a binary (yes/no) *suitable land mask*. The suitable land is then partitioned, forming a set of *candidate field plots*. The candidate field plots cover the entire suitable land area and the remaining task is to select the final set of field plots that are considered to be used for agriculture. To do so, the average suitability index is calculated for each field plot from the suitability index dataset and the field plots are selected in the suitability order, from the most suitable to least suitable. The outline of the entire field plot delineation procedure is shown in Figure 2-48 and further details of the algorithm are given in the remainder of this section.

To generate candidate field plots, all suitable land is identified first. Because the suitability index is crop-specific, the suitability for all defined crops is calculated and any raster cell whose suitability is greater than zero for any crop type is considered suitable for cultivation. The result is a binary suitable land mask containing values one (can be cultivated) and zero (cannot be cultivated). The suitable land mask is then divided into segments based on pixel connectivity so that individual segments are separated at narrow connections, as shown in Figure 2-49. The aim of the initial splitting is to divide large patches of suitable land into more compact segments, which are then processed separately.

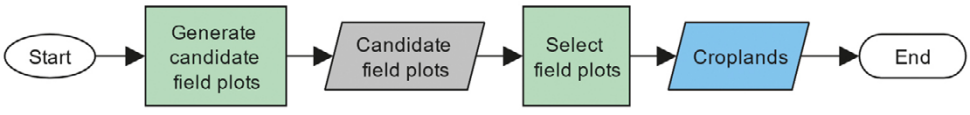

Figure 2-48. *Overview of the field plot placement algorithm. Details of the individual steps are given in the remainder of this section.*

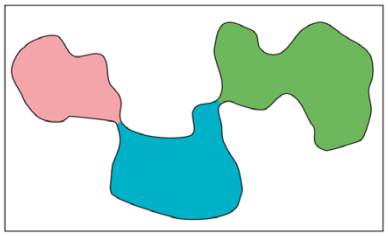

Figure 2-49. *Splitting of a large suitable land mask (shown with black outline) into three separate segments (red, green and blue).*

Subsequently, each suitable land segment is partitioned into candidate field plots as follows. First, the principal direction along which the partitioning should proceed is established. This is done by performing principal component analysis (PCA) of the geographic coordinates of all raster cells that make up the segment. The result of the PCA is the major axis along which the segment's geometry is the longest. The major axis defines the direction along which the partitioning of the segment into field plots will be carried out. To generate geometrically simple partitions, a set of points is generated along the axis at given intervals. Random noise is added to the location of the points to produce slightly irregular field plots rather than exact rectangles. Then, all pixels in the processed land segment are clustered by proximity to the generated points, resulting in a set of Thiessen polygons (Longley et al. 2005) that partition the land segment. The principal axis and generated partitions are shown in Figure 2-50, top. Partitions (polygons) which are larger than the desired area limit (parameter Agri.TargetArea) are iteratively processed further (along their own principal axes) until the desired area limit for a field plot is met. The second partitioning iteration is shown in Figure 2-50, middle and the final candidate field plots in Figure 2-50, bottom. The algorithm for generating candidate field plots is shown in Figure 2-51.

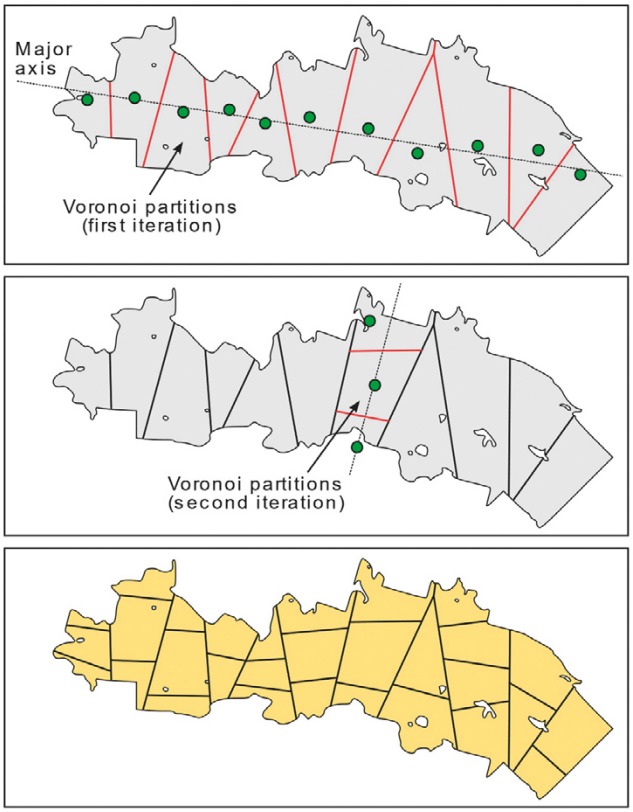

Figure 2-50. *Partitioning of a suitable area (shown in grey color) into individual field plots. Top) Partitioning of the suitable area along the major axis (axis of the first iteration). Partitioning nodes are shown as green dots, corresponding boundaries are shown in red. Middle) Second iteration in which partitions generated during the previous iteration are partitioned further. Bottom) Final generated candidate field plots.*

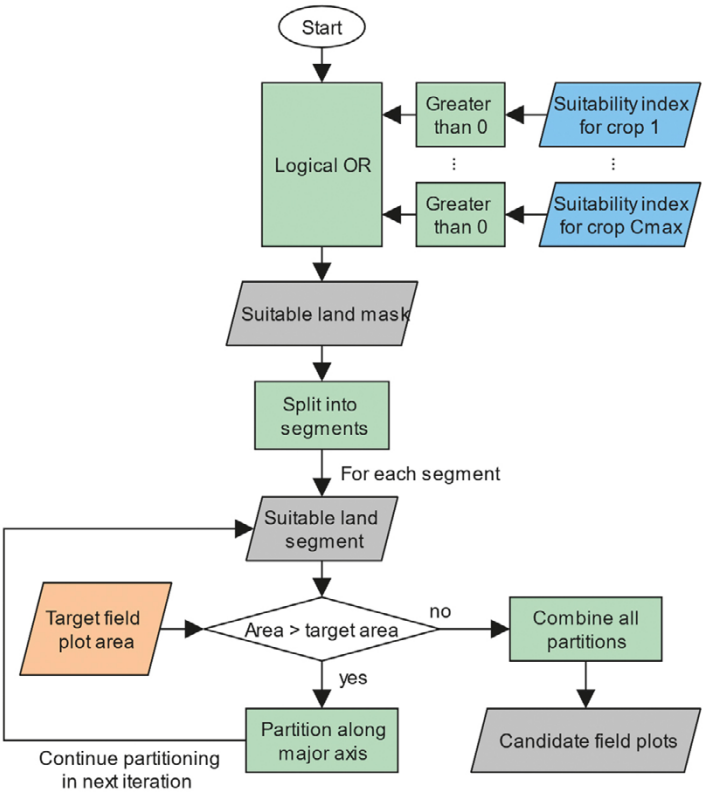

Figure 2-51. *Generation of candidate field plots.*

Once candidate field plots are generated, the allocation procedure selects final field plots from the candidate set. The selection is done for each defined crop type separately, starting from the crop with highest allocation priority (parameter Agri.LandAllocationOrder). To select field plots for given crop type, the average crop type -specific suitability index is computed for each candidate field plot which has not yet been assigned to a crop. Candidate field plots are then assigned for cultivation in their suitability order, from most to least suitable, until the allocation area target (the Agri.AllocatedLandFraction parameter) for the crop type is satisfied. Afterwards, the algorithm proceeds to allocate field plots for the next crop type in the allocation order until field plots for all crop types are allocated. The result of the field plot selection procedure is shown in Figure 2-52. The selection algorithm is shown in Figure 2-53.

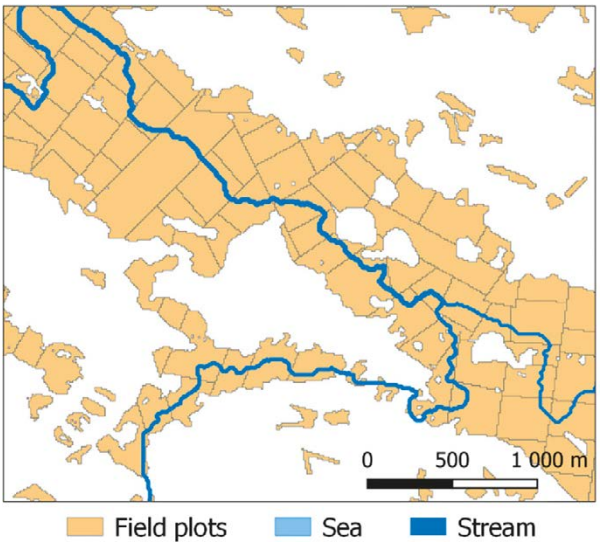

Figure 2-52. *Example of field plots allocated by UNTAMO.*

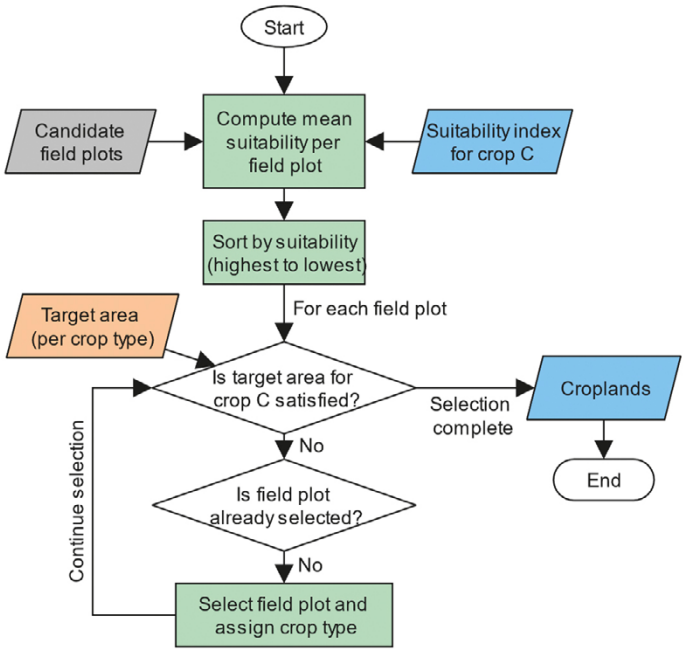

Figure 2-53. *Field plot selection for a single crop type (denoted C in the flowchart).*

It should be noted that UNTAMO can be configured to either allocate completely new set of field plots at every time step or preserve field plots selected at earlier time steps using the Agri.KeepExistingCropland parameter. Only the former approach is included in the algorithm flowcharts presented above for clarity. To preserve field plots selected at earlier time steps, the algorithm is slightly modified by setting the suitability index of areas that are in agricultural use in the previous time step to zero. This in turn prevents generation of new candidate field plots in these areas. When applying the target area constraint for a given crop type, the combined area of both newly selected and existing field plots is used and the two datasets are combined at the end to produce the final set of field plots. When preserving field plots from earlier time steps, UNTAMO also allows some field plots allocated at earlier time steps to be "abandoned" if more suitable land becomes available (parameter Agri.CanAbandonOldFields). This makes the field plot allocation slightly more dynamic and generally results in more uniform field plot density on old and emerging land. Only field plots with suitability index below given suitability limit (parameter Agri.RemovedFieldMaxSuitability) can be potentially abandoned. When more suitable land becomes available and there are fields with suitability lower than the abovementioned limit, they are removed from the field plot set to allow new field plots to be allocated within the maximum allocation limit.

The purpose of allowing existing field plots to be reused is to avoid abrupt changes occurring in the landscape from one time step to the next. This can be beneficial when modelling radionuclide transport through the landscape and ecosystem using a compartment-based model that assumes static "geometry" of the compartments (i.e. the geographic boundary of the radionuclide transport model compartments is fixed throughout the modelled time frame). However, if this is not needed, allowing UNTAMO to allocate new set of field plots at every time step may be the preferred option.

2.3.6.2 Mire drainage module

Drainage of mires results in the lowering of the terrain surface due to the removal of water and subsequent compaction of the peat column. For areas that are situated close to a water body such as a lake, drainage may not be feasible as doing so would bring the area underwater. UNTAMO detects these situations and land that cannot be drained is masked out from the areas considered for drainage. The entire algorithm for identifying non-drainable areas is shown in Figure 2-54.

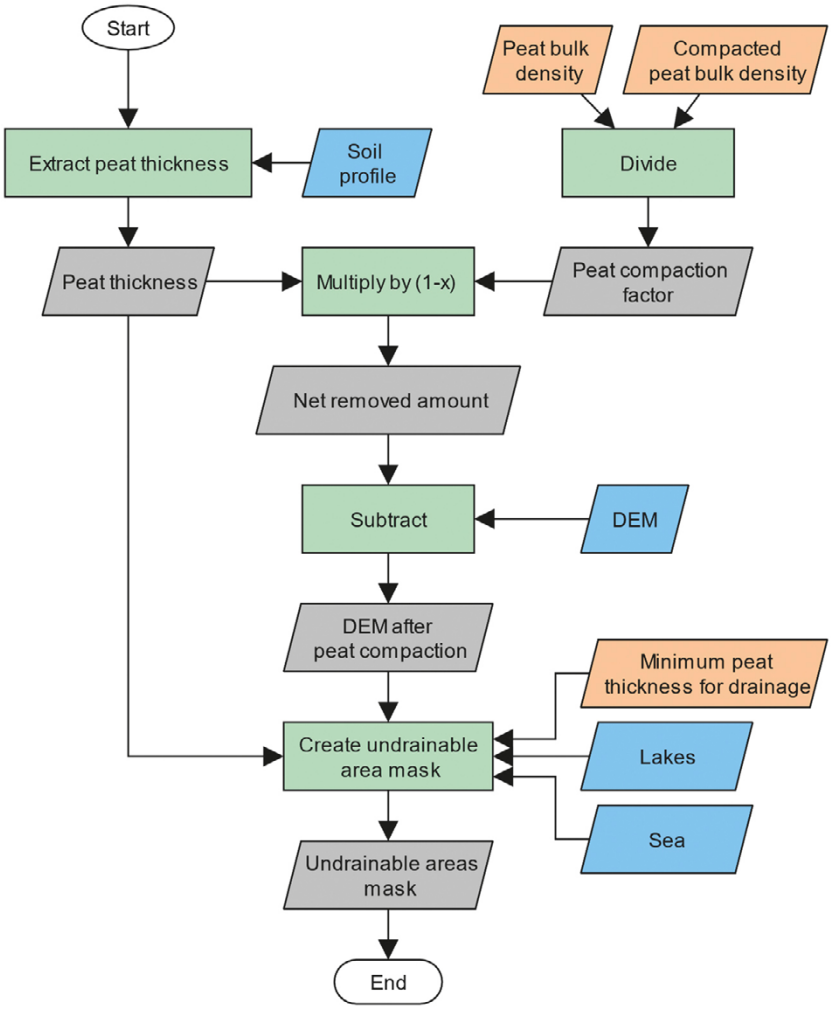

Figure 2-54. *Identification of areas that cannot be drained because doing so would lower the area below the water level of an adjacent lake or sea.*

Drainage is implemented in UNTAMO for the conversion of mires into agricultural or forest lands. To allow mire drainage for agriculture, both the drainage of mires and the use of the agricultural land allocation module (Section 2.3.6.1) must be enabled via the parameter settings. The drainage of mires for agriculture is then applied to all mires that were selected for cultivation by the agricultural land allocation module. For all mire locations that have been converted to a field plot, following changes are made to the soil profile and DEM:

- The compaction of the peat soil is realized by setting the thickness of the natural peat layer in the soil model to zero and adding the equivalent compacted thickness to the layer of compacted peat in the soil model (Figure 2-55). The compacted thickness is derived by multiplying the thickness of the natural peat layer with a compaction factor.
- The compaction factor is defined as the ratio between the user-specified bulk densities of compacted and natural peat.
- The difference between the original and the compacted peat soil thickness is also removed from the terrain elevation in the DEM, in order to keep the DEM in line with the soil model.

Drainage of mires for agriculture can be prevented by setting the suitability of peat for agriculture to zero.

Mire drainage for forestry is enabled by default and is controlled by the maximum area of natural-state (undrained) mires, given as a fraction of the total dry land. The module first performs mire drainage for agriculture, if enabled. If thereafter the natural mire area is still higher than the given maximum limit, a part of the mire is drained and converted into forest. By default, mires to be drained are selected based on the peat depth so that shallower mires are drained first. This follows an assumption that young shallow mires are easier to drain than older mires that have thicker peat deposits. Alternatively, mires to be drained can be selected randomly but the usefulness of this setting is rather limited. The process applied in UNTAMO for compacting the peat soil layer is identical to that of mire drainage for agriculture as described above.

The complete algorithm used for peatland drainage for agriculture or forestry is shown in Figure 2-56.

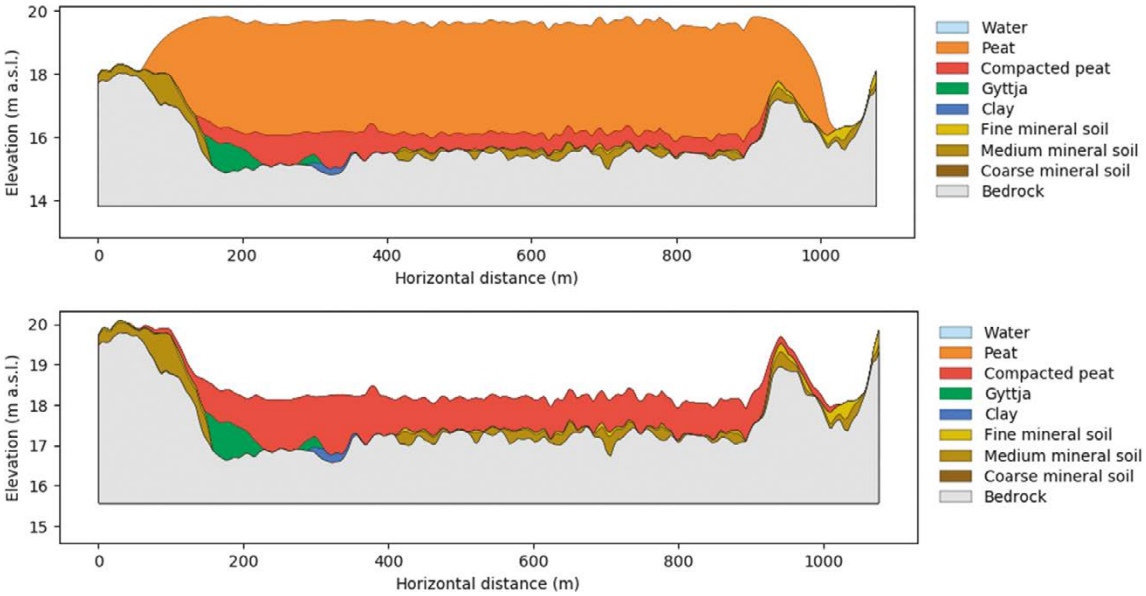

Figure 2-55. *Example of a soil cross-section before (top) and after (bottom) mire drainage. The peat layer (shown in orange) becomes compacted and the peat mass is assigned to the compacted peat layer (shown in red).*

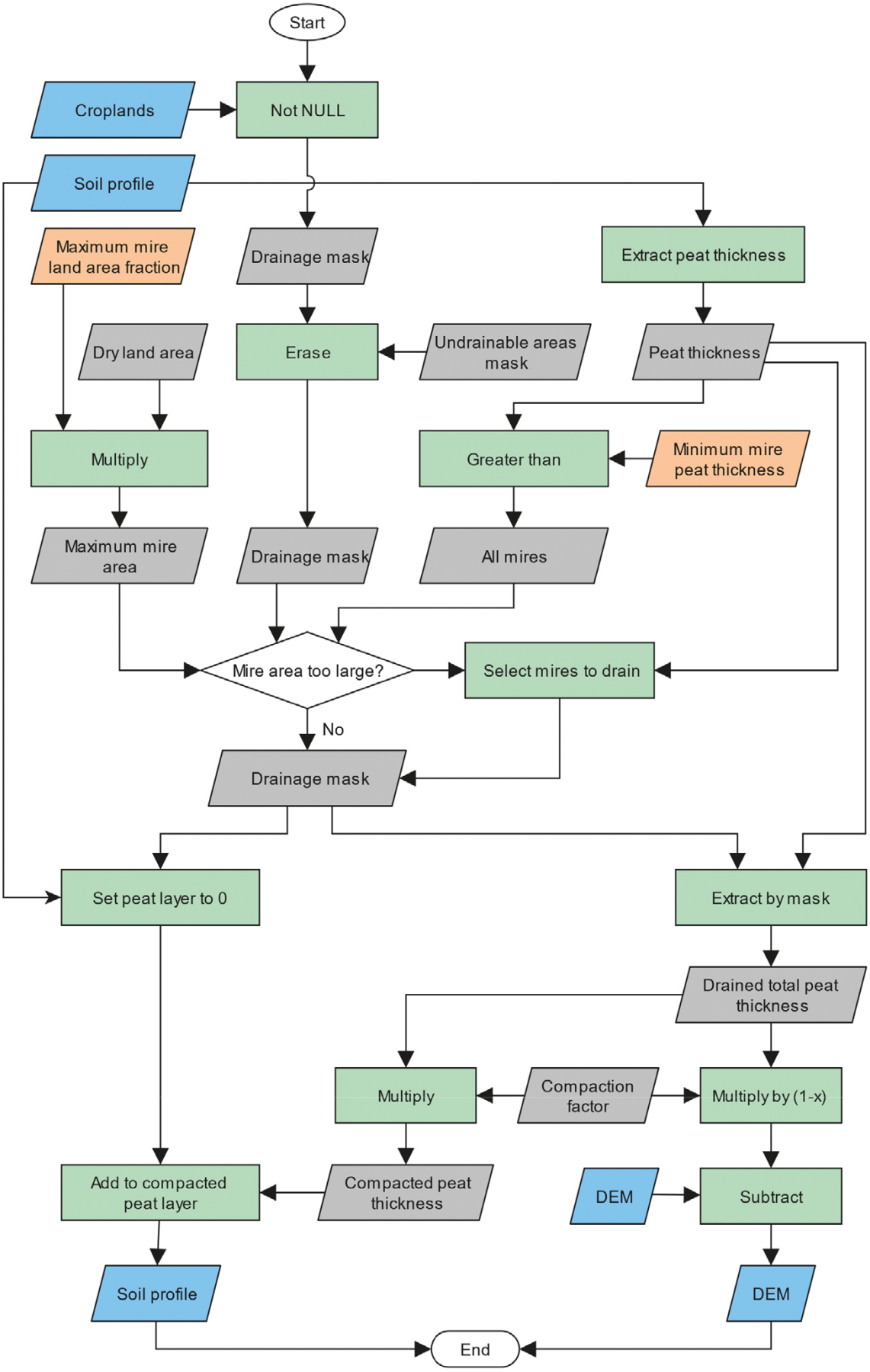

Figure 2-56. *Drainage of mires for conversion into cropland or forest.*

2.3.7 Forest sub-type classification

The forest ecosystem consists of four sub-types: rocky forest, heath forest, grove forest and mire as defined in Section 2.1.1.5. The forest sub-types are classified based on the overall sediment thickness and the dominant sediment type at the surface. Areas with total sediment thickness below the limit for thin soils (ForestSite.ThinSoilThreshold parameter) are classified as rocky forest. Areas with peat layer (both natural and compacted) thickness greater than the peat thickness limit for mire classification (MinPeatlandPeatThickness parameter) are classified as mire. Remaining areas are assigned to either heath forest or grove based on the surface sediment type, the mapping form soil type to forest sub-type can be configured using the ForestSite.ClassBySoil parameter. The forest sub-type classification is shown in Figure 2-57.

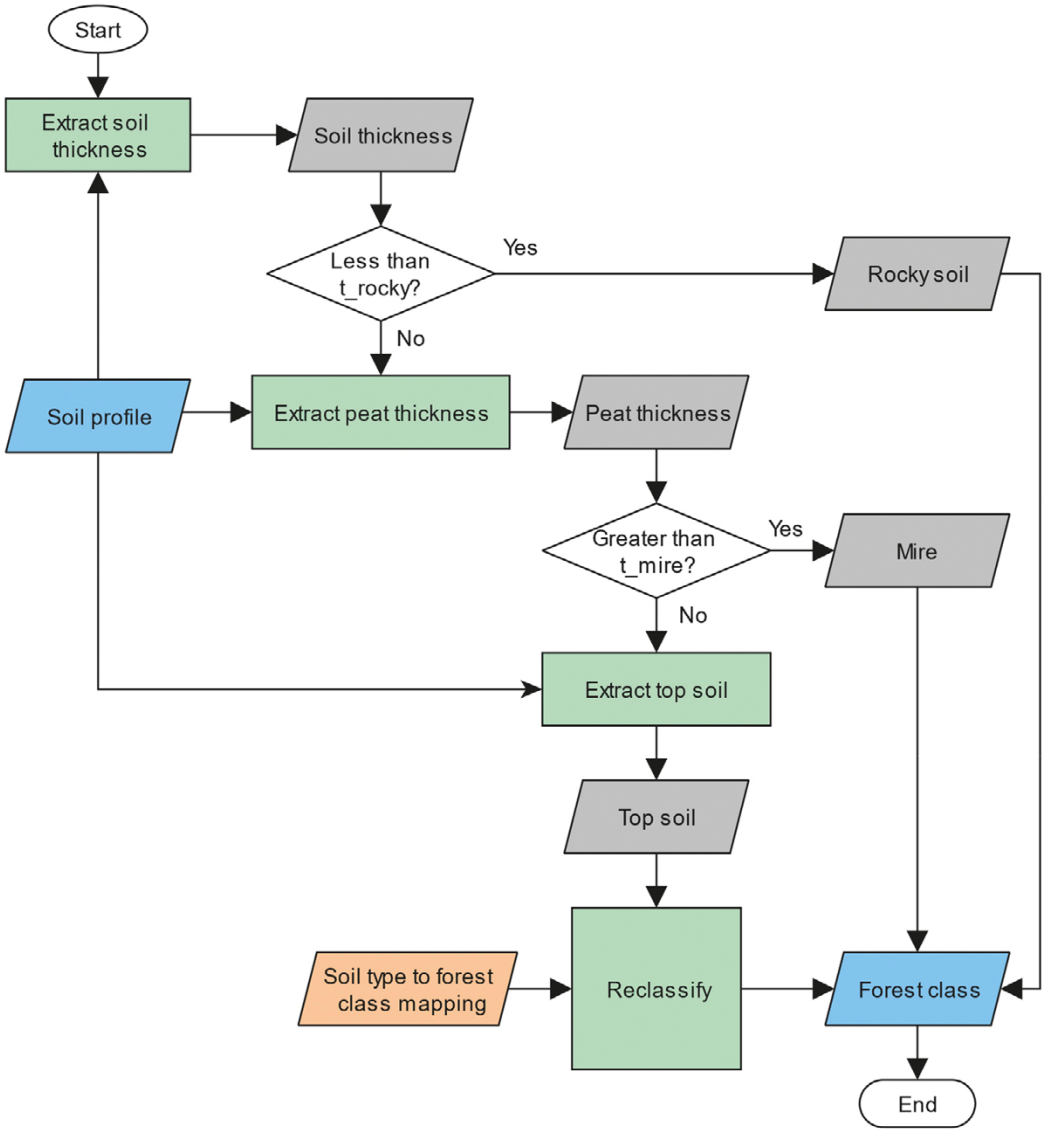

Figure 2-57. *Forest type classification based on soil stratigraphy data.*

3 Input and output documentation

3.1 Input datasets

3.1.1 Data for the initial condition

3.1.1.1 DEM

Digital elevation model raster representing terrain elevation relative to the sea level. The raster dataset must have floating point data type, the unit of the pixel values is meter above sea level (m a.s.l.). The DEM must cover the entire model grid, including areas that are currently under the sea. NoData pixels in the DEM dataset will result in the model grid cell not being modelled at all.

3.1.1.2 Soil (regolith) stratigraphy

The soil profile needs to be provided as a multi-band raster that defines the thickness (unit meter) of the individual soil layers at the beginning of the simulation. The first band represents the thickness of the top-most sediment soil type, the second band defines the thickness of the sediment layer directly beneath etc. (see Section 2.2.3). If a particular soil layer does not exist at a given location, the corresponding pixel should be set to zero thickness.

UNTAMO requires the soil profile to consist of *at least* 4 raster layers representing the following soil types: peat, gyttja/clay, mineral soil, and bedrock.

3.1.1.3 Croplands

The existing agricultural areas at the present time are to be provided as an integer raster. The raster needs to contain a unique value for each field plot and NoData elsewhere. The raster must have an attribute table with a field called CROPNAME specifying the cultivated crop type.

3.1.1.4 Mires

Existing mires are to be provided as integer raster. For each peatland, the pixel values should contain the time of formation of the mire in calendar years. UNTAMO uses the mire age to estimate the thickness of the accumulated peat. Pixels that are not located in a mire should be set to NoData.

3.1.2 Other data

3.1.2.1 Sea marker points

The sea marker points support the delineation of sea areas during the modelling. They are provided as a point vector layer where each separate sea area should have at least one point located inside. Based on the points, UNTAMO can distinguish sea areas from lakes or land areas with an elevation below the sea level.

3.1.2.2 Discharge boundary condition

External sources of discharge are to be provided as a point vector layer that mark locations at the model area boundary where main rivers enter the modelled area, that means where the modelled area receives a significant discharge from outside the area. The amount of discharge at each point is defined in the parameter file of the simulation.

3.2 Output datasets

3.2.1 Main outputs

3.2.1.1 DEM

Digital elevation model. The dataset contains elevation of the terrain surface for terrestrial ecosystems and the elevation of sea floor or lake bottom or river channel bottom for aquatic ecosystems. For mires, the elevation is taken at the surface, i.e. at the top of the peat layer.

3.2.1.2 FlowAcc(MQ, MHQ, MNQ, HQ)

Raster layers that define the accumulated discharge (unit m^3/s) at each location for the following discharge parameters:

- Mean discharge (MQ)
- Mean highest discharge (MHQ)
- Mean lowest discharge (MNQ)
- Highest discharge (HQ)

3.2.1.3 FlowDir

Raster layer defining the direction of the surface water flow at each location of the modelled area.

3.2.1.4 Sea

Raster layer which shows the areas classified as sea.

3.2.1.5 Lakes

Raster layer which shows the areas classified as lakes. Each lake has a unique pixel value and associated attributes in the raster's attribute table.

3.2.1.6 Streams

Raster layer containing individual stream segments. Each segment has a unique pixel value, and the associated attributes of each segment are stored in the raster's value attribute table.

3.2.1.7 Reed

Raster layer which shows where reed vegetation grows.

3.2.1.8 SoilProfile

Multiband raster where each band shows the thickness of one soil layer. The band order (soil layer order) matches that of the input soil profile raster (see Sections 2.2.3 and 3.1.1.2).

3.2.1.9 Cropland

Raster layer which shows the allocated field plots. Each field plot has a unique pixel value and the associated attributes are stored in the raster's attribute table.

3.2.2 Additional outputs

The additional output raster layers listed below are side products of the simulation which allow a more in-depth check of the simulation results.

3.2.2.1 DtmHillshade

Raster layer showing the hillshade view of the terrain. This output is only relevant for presentation purpose, for example as a background layer for a map showing simulation results.

3.2.2.2 Site

Raster layer showing the ecosystem sub-types for all areas that have been classified as forest ecosystem (see Table 2-1). The sub-types are assigned based on the surface sediment type. Each sub-type has a unique pixel value. The code values are defined as follows: 0 = rocky forest, 1 = heath forest, 2 = herb-rich forest, 3 = mire.

3.2.2.3 SoilThickness

Raster layer showing for each location the total soil thickness, i.e. the thickness of all soil layers combined.

3.2.2.4 TopSoil

Raster layer showing for each location the top-most sediment type. Each sediment type is represented by a code value which is identical with the index (band number) of the corresponding sediment type in the input soil profile raster (see Section 3.1.1.2).

3.2.2.5 PeatBases

Raster layer showing areas with peat soil. Each pixel value represents the formation year (age) of the peat soil in that particular location.

3.2.2.6 WaterDepth

Raster layer representing the depth of the water column (unit meters) for lake and sea areas.

3.2.2.7 SDMErDep

Raster layer representing for each location the net change in sediment thickness since the simulation start year. Positive pixel values indicate a net accumulation of sediment while negative values represent net erosion.

3.2.2.8 SDMBottomClass

Raster layer showing the sea and lake areas classified by three categories that characterize the prevailing sediment dynamics at each location: Erosion bottom (pixel value 1), accumulation bottom (pixel value 2), and transition zone (pixel value 0).

3.2.2.9 SDMDurationAcc

Raster layer representing the total amount of years during which a location has experienced sediment accumulation since the simulation start year.

3.2.2.10 SDMDurationEr

Raster layer representing the total amount of years during which a location has experienced sediment erosion since the simulation start year.

3.2.2.11 ChannelErAmount

The erosion amount (unit meters) that UNTAMO applies to the digital elevation model and soil profile at all locations that are part of the stream network. The amount is derived based on the highest discharge (HQ) for each stream location. The eroded volume equals the required stream channel volume to accommodate the highest discharge.

3.2.2.12 CropSuitability

Raster layer showing which areas are suitable for the cultivation of crops based on the suitability criteria applied by UNTAMO (Section 2.3.6.1). This raster is different from the 'Cropland' output raster since only a part of the suitable areas are selected as croplands. In other words, the allocated croplands are a subset of the areas suitable for crop cultivation. A pixel value of 1 indicates areas suitable for crop cultivation and a pixel value of zero represents non-suitable areas.

4 Potential for future development

Several areas of potential for future work have been identified. The documentation of the UNTAMO model (this document) could be improved and extended further, by providing additional details of the implemented algorithms and improving clarity. All parameters of the model should also be documented in the future.

Furthermore, some issues with the model conceptualization and implementation have been raised and should be addressed. As an example, the use of the Manning formula for estimation of stream channel geometry in Section 2.3.3.3 is seen as problematic and should be revised. The rate of in-filling of lakes by littoral vegetation in the current implementation of the sediment dynamics module is also known to require more testing and development. The extent of the littoral zones, and consequently the rate at which lakes are in-filled, depends on the geometry of the lake shoreline. The current algorithm is known to converge to rather round-shaped lakes over time and the rate of in-filling decreases.

Another area of improvement would be to streamline the UNTAMO model. The model has been in development over more than a decade and several models and algorithms were tested but discontinued over time. It would therefore be beneficial to identify and remove execution paths that are no longer used. This would simplify both the setting up and documentation of the model. Parameters of the UNTAMO models could also be revisited with the aim to increase clarity of what they represent and how they should be used.

New modules may also be added to the UNTAMO software, for example more advanced algorithm for identification of wetlands that has been under research at SKB.

References

SKB's (Svensk Kärnbränslehantering AB) publications can be found at www.skb.com/publications.

Brydsten L, Strömgren M, 2013. Landscape development in the Forsmark area from the past into the future (8500 BC–40,000 AD). SKB R-13-27, Svensk Kärnbränslehantering AB.

Clymo R S, 1984. The limits to peat bog growth. Philosophical Transactions of the Royal Society of London, Series B 303, 605–654.

Coastal Engineering Research Center, 1984. Shore protection manual, Vol. 1. Coastal Engineering Research Center, Department of the Army, Waterways Experiment Station, Corps of Engineers.

Gunia M, Gunia K, 2022. Calibration and validation of UNTAMO submodels for TESM in SC-OLA. Posiva Working Report 2021-26, Posiva Oy, Finland.

Hjerpe T, Ikonen A T K, Broed R, 2010. Biosphere assessment report 2009. Posiva 2010-03, Posiva Oy, Finland.

Huikari O, 1956. Primäärisen soistumisen osuudesta Suomen soiden synnyssä (in Finnish with a German abstract: Untersuchungen Über den Anteil der Primären Versumpfung an der Entstehung der Finnischen More; On the role of primary mire formation in Finland). Communicationes Instituti Forestalis Fenniae 46, 1–79.

Jenson S K, Domingue J O, 1988. Extracting topographic structure from digital elevation data for geographic information system analysis. Photogrammetric Engineering and Remote Sensing 54, 1593–1600.

Kivinen E, 1948. Suotiede (Peatland science). Porvoo, Finland: WSOY. (In Finnish.)

Komar P D, Miller M C, 1972. The threshold of sediment movement under oscillatory water waves. Journal of Sedimentary Research 43, 1101–1110.

Korhola A, Tolonen K, 1996. The natural history of mires in Finland and the rate of peat accumulation. In Vasander H (ed). Peatlands in Finland. Helsinki: Finnish Peatland Society, 20–26.

Leopold L B, Maddock T, 1953. The hydraulic geometry of stream channels and some physiographic implications. Washington, DC: U.S. Government Printing Office.

Longley P A, Goodchild M F, Maguire D J, Rhind D W, 2005. Geographic information systems and science. 2nd ed. Chichester: Wiley.

Manning R, Griffith J P, Pigot T F, Vernon-Harcourt L F, 1890. On the flow of water in open channels and pipes. Transactions of the Institution of Civil Engineers of Ireland 20, 161–207.

Mulvany T, 1851. On the use of self-registering rain and flood gauges in making observations of the relations of rain fall and flood discharges in a given catchment. Transactions of the Institution of Civil Engineers of Ireland, 4, 18–33.

NLS, 2022. Open data file download service. National Land Survey of Finland (NLS). Available at: https://www.maanmittauslaitos.fi/en/e-services/open-data-file-download-service

Planchon O, Darboux F, 2002. A fast, simple and versatile algorithm to fill the depressions of digital elevation models. Catena 46, 159–176.

Posiva, 2013. Safety case for the disposal of spent nuclear fuel at Olkiluoto. Terrain and ecosystems development modelling in the Biosphere assessment BSA-2012. Posiva 2012-29, Posiva Oy, Finland.

Påsse T, 2001. An empirical model of glacio-isostatic movements and shore-level displacement in fennoscandia. SKB R-01-41, Svensk Kärnbränslehantering AB.

Ramanujan A S, Hardy G H (ed), Seshu Aiyar P V (ed), Wilson B M (ed), 1962. Collected papers of Srinivasa Ramanujan. New York: Chelsea.

Syvitski J P, Morehead M D, Bahr D B, Mulder T, 2000. Estimating fluvial sediment transport: The rating parameters. Water Resources Research 36, 2747–2760.

Tarboton D G, 1997. A new method for the determination of flow directions and upslope areas in grid digital elevation models. Water Resources Research 33, 309–319.

Tolonen K, 1977. On dry mater accumulation and bulk density values in three south Finnish raised bogs. Suo 28, 1–8.

Arkitektkopia AB, Bromma, 2022

SKB is responsible for managing spent nuclear fuel and radioactive waste produced by the Swedish nuclear power plants such that man and the environment are protected in the near and distant future.

skb.se